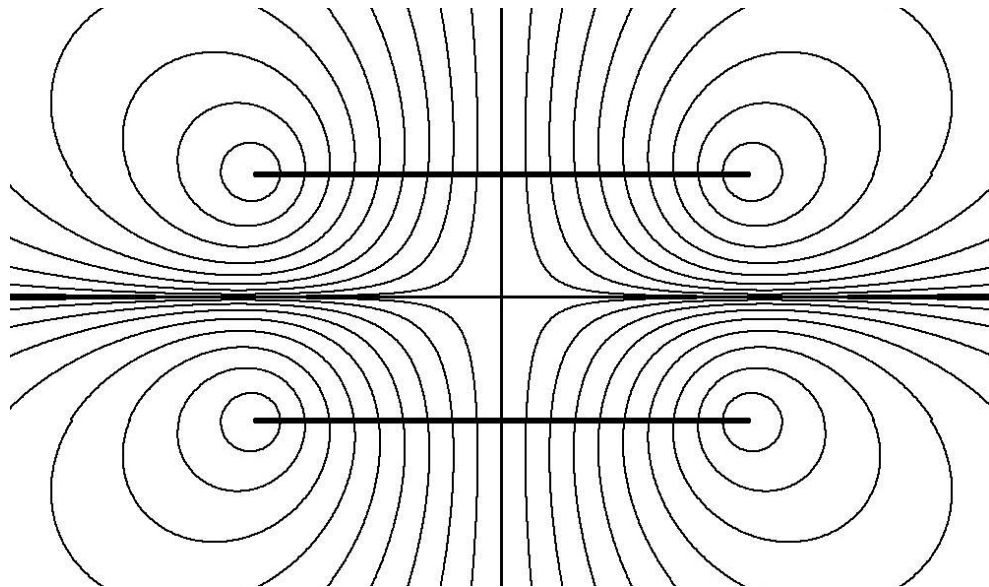




The Elliptical Lead Zeppelin



THESIS

submitted in partial fulfillment of the
requirements for the degree of

BACHELOR OF SCIENCE

in

PHYSICS

Author :	I.R. Berkman
Student ID :	1230638
Supervisor :	Prof. Dr. Ir. T.H. Oosterkamp
2 nd corrector :	Prof. Dr. M. Allan

Leiden, The Netherlands, August 18, 2015

The Elliptical Lead Zeppelin

I.R. Berkman

Huygens-Kamerlingh Onnes Laboratory, Leiden University
P.O. Box 9500, 2300 RA Leiden, The Netherlands

August 18, 2015

Abstract

A new dipstick is built for the Lead Zeppelin project but with elliptical coils. We want to find the harmonic potential of this new configuration.

Contents

1	Introduction	1
1.1	MRFM	1
1.2	New Sensors using Magnetic Levitation	1
1.2.1	Benefits of using Elliptical Coils	2
1.3	Goals	2
2	Theory	3
2.1	Magnetic Fields	3
2.1.1	Magnetic Flux	3
2.1.2	The Biot-Savart Law	5
2.1.3	On-Axis Magnetic Field of Circular Coils in an AH-Configuration	5
2.1.4	Off-axis Magnetic Field of Circular Coils in an AH-Configuration	8
2.1.5	Off-axis Magnetic Field of Elliptical Coils in an AH-Configuration	10
2.2	Superconductivity	12
2.2.1	Characteristics of Superconductors	12
2.2.2	Superconductor in a Magnetic Field	12
2.2.3	Resonance Frequencies of a Sphere	13
2.2.4	Resonance Frequencies of a Cube	14
2.2.5	Mixing Frequencies	16
2.2.6	Double Frequencies	19
3	Materials and Methods	21
3.1	The Circuit	21
3.1.1	The Scheme	21

3.1.2	The Switch	22
3.1.3	Twisting Wires	24
3.2	The Elliptical Coils	26
3.2.1	Winding the Coils	26
3.2.2	Assembling the Coils	28
3.3	The Big Coil	30
3.3.1	The Machine	30
3.3.2	Making the Big Coil	31
3.4	The Lead Particles	34
3.5	Preparing the Dipstick	36
4	Numerical Calculations and Predictions	41
4.1	The Magnetic Field	41
4.2	Approximating the Magnetic Field	47
4.3	Resonance Frequencies	50
4.3.1	Translational Frequencies	50
4.3.2	Rotational Frequencies	52
5	Results and Discussion	53
5.1	The Lead Zeppelin Experiment	53
5.2	Numerical Results	54
5.3	Fourier Spectrum of the Spherical Lead Zeppelin with Circular Coils	55
6	Conclusions	59
7	Follow up Experiments and Improvements	61
8	Acknowledgements	63

Introduction

1.1 MRFM

Magnetic Resonance Force Microscopy (MRFM) is a technique which uses Atomic Force Microscopy (AFM) and Magnetic Resonance Imaging (MRI) to obtain images at nanometer scales.

The MRFM technique uses an ultrathin silicon cantilever with a ferromagnetic (iron cobalt) tip. Because an electron has a magnetic property called "spin", it can attract or deflect the magnetic tip depending on the spin-position. The spins are repeatedly flipped by a high-frequency magnetic field induced by a coil. The result is that the cantilever oscillates due to the repelling and attracting forces of the flipping spins. By monitoring the cantilever oscillation with an interferometer while the sample moves underneath the cantilever creates data for a two of three dimensional reconstruction. These measurements are usually performed at low temperatures to reduce the noise of Brownian motions[1].

1.2 New Sensors using Magnetic Levitation

Because we are measuring particles on a nanoscale, we can conclude that the corresponding forces are very small and in this case in the order of zeptonewtons. Any loss of energy will have an influence on the very sensitive detecting systems. The MRFM technique loses energy on bending

the cantilever, therefore the measurements will be more accurate when these energy losses are decreased or even better, removed.

A ingenious solution was published by Romero-Isart in his article “Quantum Magnetomechanics with Levitating Superconducting Microspheres”[2]. A superconducting particle is trapped in an anti-Helmholtz configuration. Because the potential is zero in the middle of the configuration, the superconductor tends to stay there due to the Meissner effect[3]. This system has no mechanical energy losses which allows it to have a higher Q factor, a measure for the quality of an oscillating device, than ever before. More information about specifically these kinds of sensors can be found in “The Lead Zeppelin Project” by M. De Wit[4].

1.2.1 Benefits of using Elliptical Coils

The original Lead Zeppelin project consisted of a small spherical piece of lead trapped in between two circular coils with repelling magnetic fields. The lead in this system has 6 degrees of freedom, where three are translational and three rotational. Because the field is symmetric in the $x=0$ and $y=0$ plane it becomes hard to distinguish the two translational frequencies in the x and y direction. Also, due to symmetry, the rotational frequency is immeasurable. This is more thoroughly explained in the “Theory” chapter.

A way to distinguish the translational frequencies better is by making the magnetic field more asymmetrical. The most practical form is the elliptic one, which is just a squeezed circle. By using two elliptical coils we can now find which frequencies correspond to the translation frequency in the x and y direction. The rotational frequencies can be found by making the Zeppelin aspherical.

1.3 Goals

- Making the Lead Zeppelin with elliptical coils
- Finding the corresponding frequencies
- Finding the Q factor
- Making the Lead Zeppelin aspherical

Chapter 2

Theory

2.1 Magnetic Fields

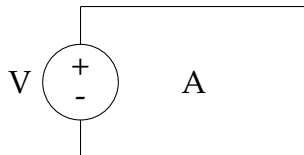
2.1.1 Magnetic Flux

Flux is a key concept when talking about magnetic fields. In electromagnetism, the magnetic flux Φ is the surface integral of the normal component of the magnetic field \vec{B} passing through that surface, or in equation-form:

$$\Phi = \iint \vec{B} \cdot d\vec{S} \quad (2.1)$$

When reading through this thesis, you will often find the word "twisted wires" and this has everything to do with flux.

Say, for instance, that we have a closed circuit with area A.



Every electromagnetic noise (cellphones, transmission lines, fluorescent light etcetera) will go through this area and deliver a flux. Every difference

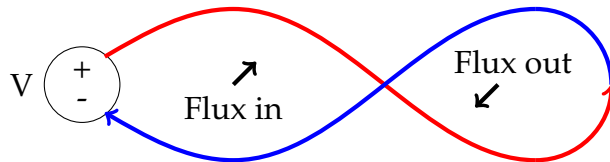
in flux will induce an electromotive force or EMF which is given by

$$\text{EMF} = -\frac{d\Phi}{dt} \quad (2.2)$$

And because EMF is measured in voltage, the total voltage over the circuit will be different than the voltage of the source.

In present-day circuits, we almost never calculate with these kind of noise fluxes because they are too small to make any significant differences. However, when we zoom in into a quantum scale these noises can become disastrous.

We can solve this by giving this wire a twist in the middle as seen below.



Let us assume that both sides have an equal area and the magnetic field is a constant. The flux is then the same on both sides. But because of the twist, the two \vec{A} vectors will have opposite sign and the fluxes will cancel, resulting in a zero EMF.

In reality it is much harder to twist the wire exactly in the middle and keeping the areas in the same plane. It then becomes more practical to just twist the wires as tightly as possible.

2.1.2 The Biot-Savart Law

The Biot-Savart Law helps us calculating magnetic fields. Almost all the equations in this experiment can be derived from this law:

$$\vec{B}(\vec{r}) = \frac{\mu_0}{4\pi} \int \frac{\vec{I} \times \hat{r}}{r^2} dl' = \frac{\mu_0}{4\pi} I \int \frac{d\vec{l}' \times \vec{r}}{r^3} \quad (2.3)$$

Where the constant μ_0 is called the permeability of free space:

$$\mu_0 = 4\pi \times 10^{-7} \text{ N/A}^2 \quad (2.4)$$

The integration is along the path of the current \vec{I} . This path consists of the infinitesimal small $d\vec{l}'$. The script r " \vec{r} " is the vector from the current source to the point \vec{r} . The resulting magnetic field is given in Tesla.

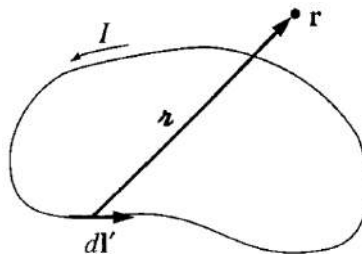


Figure 2.1: The elements of the Biot-Savart law in a sketch taken from Griffiths' "Introduction to Electrodynamics"[5]

2.1.3 On-Axis Magnetic Field of Circular Coils in an AH-Configuration

One of the easiest examples of the Biot-Savart law (equation 2.3) in use is the on-axis magnetic field of a round current loop.

We want to find the magnetic field a distance z above the center of a circular loop of radius R , which carries a steady current I (Fig. 2.2).

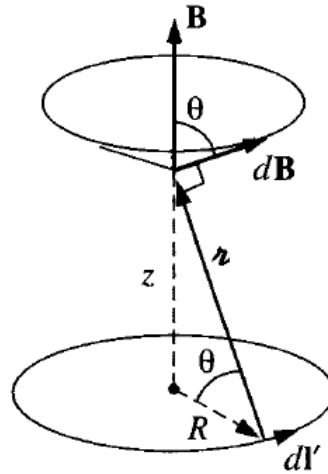


Figure 2.2: The elements for calculating the on-axis magnetic field of a circular current loop

The cross product of $d\vec{l}'$ and \vec{r} is in the direction of the $d\vec{B}$ as shown in the figure. As we integrate $d\vec{l}'$ around the loop, $d\vec{B}$ sweeps out a cone. Because of the circular symmetry, the horizontal components cancel and the resulting \vec{B} points only upward. This means we only have to look at the vertical component of $d\vec{B}$ which is $\cos(\theta)d\vec{B}$. The Biot-Savart law becomes

$$B(z) = \frac{\mu_0 I}{4\pi} \int \frac{d\vec{l}'}{r^2} \cos \theta = \frac{\mu_0 I}{4\pi} \left(\frac{\cos \theta}{r^2} \right) \int d\vec{l}'. \quad (2.5)$$

The $\cos \theta$ and r are constants so we place these in front of the integral, so we only have to integrate over $d\vec{l}'$. The path is over a circle so the path integral becomes the circumference $2\pi R$. The field becomes:

$$B(z) = \frac{\mu_0 I}{4\pi} \left(\frac{\cos \theta}{r^2} \right) 2\pi R = \frac{\mu_0 I}{2} \frac{R^2}{(R^2 + z^2)^{3/2}}. \quad (2.6)$$

We now place two circular loops at distance $z = d$ and $z = -d$ as shown in fig. 2.3. This type of configuration is known as an "anti-Helmholtz configuration" or shortened: "AH-configuration".

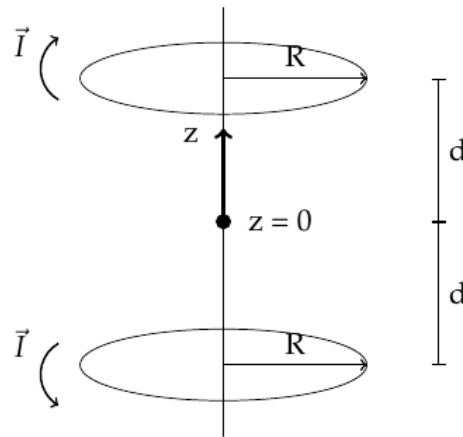


Figure 2.3: An anti-Helmholtz configuration

This means that for the loop at $z = -d$ the equation for the on-axis magnetic field (equation 2.6) will be the same except now the variable z is substituted for $z + d$. For the loop at $z = d$ the substitution will be $z - d$ and the field will be negative because of the opposite current flow.

We can then add these two magnetic fields to get the total on-axis magnetic field at distance z of the origin:

$$B(z) = \frac{\mu_0 I R^2}{2} \left(\frac{1}{(R^2 + (z + d)^2)^{3/2}} - \frac{1}{(R^2 + (z - d)^2)^{3/2}} \right) \quad (2.7)$$

We can approximate the magnetic field of a coil by overlapping the loop n times on the same position of the loop, where n is the number of windings. The equation for two opposite placed coils with both the same number of windings will then be:

$$B_{coils}(z) = n \cdot \frac{\mu_0 I R^2}{2} \left(\frac{1}{(R^2 + (z + d)^2)^{3/2}} - \frac{1}{(R^2 + (z - d)^2)^{3/2}} \right) \quad (2.8)$$

Although we want to look more at the off-axis magnetic fields, this section provides a good understanding of the mathematical properties of magnetic fields. The mathematics tend to become more difficult the more asymmetrical we get.

2.1.4 Off-axis Magnetic Field of Circular Coils in an AH-Configuration

Calculating the off-axis field of a circular loop at point \vec{r} breaks some symmetry and therefore requires more use of the elements of the Biot-Savart law (equation 2.3). We will look at the elliptical coil hereafter so it is better to calculate it in Cartesian coordinates instead of cylindrical.

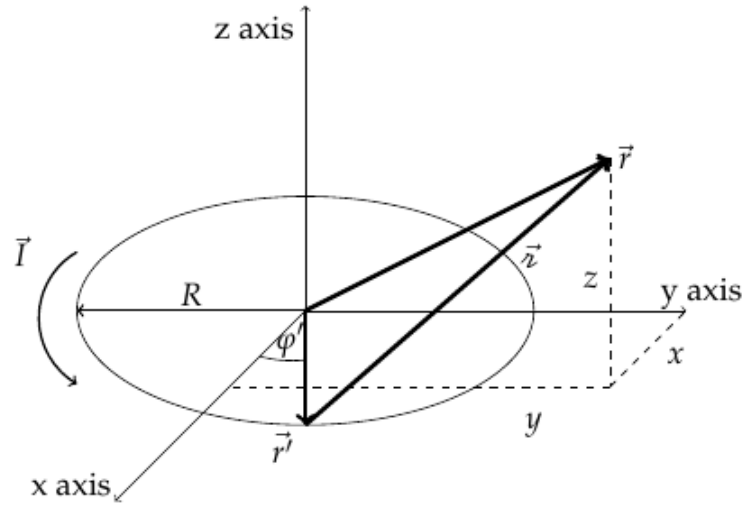


Figure 2.4: Off-axis magnetic field of a circular current loop

The point \vec{r} is where we want to calculate the magnetic field and the point \vec{r}' describes the path of the current flow. Both in Cartesian coordinates are

$$\vec{r} = \begin{pmatrix} x \\ y \\ z \end{pmatrix} \text{ and } \vec{r}' = \begin{pmatrix} R \cos \varphi' \\ R \sin \varphi' \\ 0 \end{pmatrix}. \quad (2.9)$$

A segment $d\vec{l}'$ is basically the same as $d\vec{r}'$ and can be found by $\frac{d\vec{r}'}{d\varphi'}d\varphi'$.

The vector \vec{z} is equal to the vector difference $\vec{r} - \vec{r}'$, so we get

$$d\vec{l}' = \begin{pmatrix} -R \sin \varphi' \\ R \cos \varphi' \\ 0 \end{pmatrix} d\varphi' \text{ and } \vec{z} = \begin{pmatrix} x - R \cos \varphi' \\ y - R \sin \varphi' \\ z \end{pmatrix}. \quad (2.10)$$

The integral of Biot-Savart law requires the cross product $d\vec{l}' \times \vec{r}$:

$$d\vec{l}' \times \vec{r} = \begin{pmatrix} zR \cos \varphi' \\ zR \sin \varphi' \\ R^2 - yR \sin \varphi' - xR \cos \varphi' \end{pmatrix} d\varphi' \quad (2.11)$$

and it requires r^3 :

$$r^3 = (\vec{r} \cdot \vec{r})^{3/2} = (x^2 + y^2 + z^2 + R^2 - 2xR \cos \varphi' - 2yR \sin \varphi')^{3/2} \quad (2.12)$$

Combining 2.11 and 2.12 gives us the magnetic field

$$B_x(\vec{r}) = \frac{\mu_0 IRz}{4\pi} \int_0^{2\pi} \frac{\cos \varphi'}{r^3} d\varphi' \quad (2.13)$$

$$B_y(\vec{r}) = \frac{\mu_0 IRz}{4\pi} \int_0^{2\pi} \frac{\sin \varphi'}{r^3} d\varphi' \quad (2.14)$$

$$B_z(\vec{r}) = \frac{\mu_0 IR}{4\pi} \int_0^{2\pi} \frac{R - x \cos \varphi' - y \sin \varphi'}{r^3} d\varphi' \quad (2.15)$$

We have seen in section 2.1.3 that going from one loop to two opposite placed loops is just a matter of substituting z for $z + d$ and $z - d$. The magnetic field at point \vec{r} for an anti-Helmholtz configuration with coils of n number of windings will be

$$B_x(\vec{r}) = \frac{\mu_0 IRn}{4\pi} \int_0^{2\pi} \left(\frac{(z+d)}{r_+^3} - \frac{(z-d)}{r_-^3} \right) \cos \varphi' d\varphi' \quad (2.16)$$

$$B_y(\vec{r}) = \frac{\mu_0 IRn}{4\pi} \int_0^{2\pi} \left(\frac{(z+d)}{r_+^3} - \frac{(z-d)}{r_-^3} \right) \sin \varphi' d\varphi' \quad (2.17)$$

$$B_z(\vec{r}) = \frac{\mu_0 IRn}{4\pi} \int_0^{2\pi} \left(\frac{1}{r_+^3} - \frac{1}{r_-^3} \right) (1 - xR \cos \varphi' - yR \sin \varphi') d\varphi' \quad (2.18)$$

With

$$r_+^3 = (x^2 + y^2 + (z+d)^2 + R^2 - 2xR \cos \varphi' - 2yR \sin \varphi')^{3/2} \quad (2.19)$$

$$r_-^3 = (x^2 + y^2 + (z-d)^2 + R^2 - 2xR \cos \varphi' - 2yR \sin \varphi')^{3/2} \quad (2.20)$$

2.1.5 Off-axis Magnetic Field of Elliptical Coils in an AH-Configuration

Elliptical current loops will have different field lines in the x and y direction. In figure 2.5 we see that the radius constant R for a circular loop has taken place for two constants: a and b . The constant a is the distance from the centre to the ellipse along the x axis, the constant b the distance from the centre to the ellipse along the y axis.

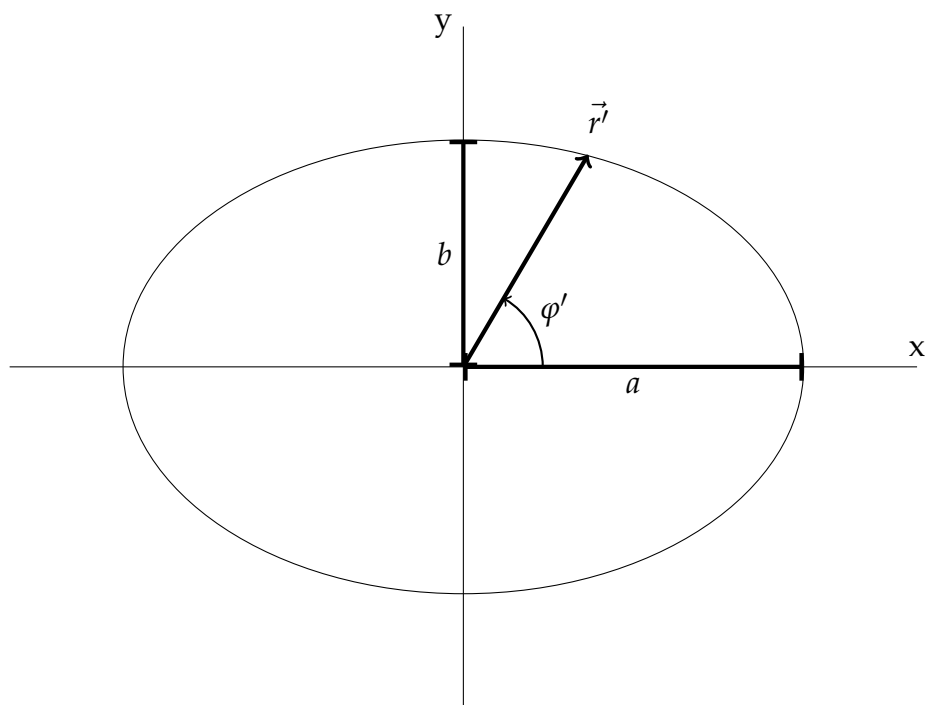


Figure 2.5: The elliptical loop in the $z = 0$ plane

The only difference in calculating the magnetic field of the elliptical loop is that the coordinates of \vec{r}' now become

$$\vec{r}' = \begin{pmatrix} a \cos \varphi' \\ b \sin \varphi' \\ 0 \end{pmatrix} \quad (2.21)$$

The whole derivation is just the same as the circular loop, so we can skip instantly to the equations for the elliptical coils in an anti-Helmholtz configuration:

$$B_x(\vec{r}) = \frac{\mu_0 I b n}{4\pi} \int_0^{2\pi} \left(\frac{(z+d)}{r_+^3} - \frac{(z-d)}{r_-^3} \right) \cos \varphi' d\varphi' \quad (2.22)$$

$$B_y(\vec{r}) = \frac{\mu_0 I a n}{4\pi} \int_0^{2\pi} \left(\frac{(z+d)}{r_+^3} - \frac{(z-d)}{r_-^3} \right) \sin \varphi' d\varphi' \quad (2.23)$$

$$B_z(\vec{r}) = \frac{\mu_0 I n}{4\pi} \int_0^{2\pi} \left(\frac{1}{r_+^3} - \frac{1}{r_-^3} \right) (ab - bx \cos \varphi' - ay \sin \varphi') d\varphi' \quad (2.24)$$

Where

$$r_+^3 = (x^2 + y^2 + (z+d)^2 + a^2 \cos^2 \varphi' + b^2 \sin^2 \varphi' - 2ax \cos \varphi' - 2by \sin \varphi')^{3/2} \quad (2.25)$$

$$r_-^3 = (x^2 + y^2 + (z-d)^2 + a^2 \cos^2 \varphi' + b^2 \sin^2 \varphi' - 2ax \cos \varphi' - 2by \sin \varphi')^{3/2} \quad (2.26)$$

Note how substituting both a and b for R gives the same equations as the circular magnetic fields.

Unfortunately, we have broken the symmetry so much that we can not derive these equations any further, even with a Taylor expansion the equations will still be troublesome. The only way to calculate the fields quickly is with computing software.

2.2 Superconductivity

2.2.1 Characteristics of Superconductors

Superconductors are elements, inter-metallic alloys, or compounds that conduct electricity with zero resistance below a certain temperature and external magnetic field.[6]

There are two types of superconductors: type I and type II. Type II usually have higher critical fields than type I superconductors.

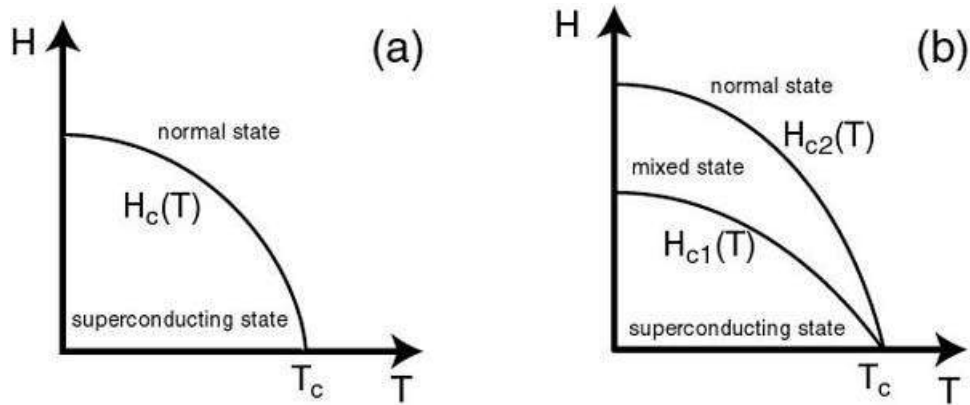


Figure 2.6: Critical magnetic field as a function of temperature for (a) type I superconductors and (b) type II superconductors. [7]

In this experiment two types of conducting wires are being used: a type II niobium and a type II niobium-titanium. Niobium has a critical temperature of 9.2 Kelvin [8] and niobium-titanium at 10 Kelvin. [9]

The particle floating in the anti-Helmholtz configuration is made of pure lead which is a type I and has a critical temperature of 7.3 Kelvin. [10]

2.2.2 Superconductor in a Magnetic Field

The total force on a superconductor in a magnetic field is given by the equation 2.27 found in "Local model for magnet-superconductor mechanical interaction: Experimental verification" by E. Diez-Jimenez et al. [11]

$$\vec{F} = \oint 2\mu_0(\vec{n} \times \vec{H})\vec{H} dS. \quad (2.27)$$

Where the surface integral encloses the surface of the superconducting particle. The vector \vec{n} is the normal on the surface and \vec{H} is the magnetic field strength $\vec{H} = \vec{B}/\mu_0 - \vec{M}$, where \vec{B} is the extern magnetic field. We work in vacuum so we assume $\vec{M} = 0$ which results in a magnetic field $\vec{B}_{ext} = \mu_0\vec{H}_{ext}$.

Equation 2.27 can then be rewritten as:

$$\vec{F} = -\frac{2}{\mu_0} \oint \left[\vec{n} \|\vec{B}\|^2 - \vec{B}(\vec{n} \cdot \vec{B}) \right] dS. \quad (2.28)$$

2.2.3 Resonance Frequencies of a Sphere

The force on a spherical particle in an anti-Helmholtz configuration with circular coils has been calculated in the thesis "Beweging van een supergeleidende bol in een anti-Helmholtz-configuratie by T. de Jong and D. Kok.[12]

$$\vec{F}(r, z) = -\frac{6\pi a^3 \mu_0 n^2 I^2 R^4 d^2}{(R^2 + d^2)^5} (r\hat{r} + 4z\hat{z}) \quad (2.29)$$

This is equal to the equation of motion of an harmonic oscillator. The spring constants are:

$$k_r = \frac{6\pi a^3 \mu_0 n^2 I^2 R^4 d^2}{(R^2 + d^2)^5} \text{ and } k_z = \frac{24\pi a^3 \mu_0 n^2 I^2 R^4 d^2}{(R^2 + d^2)^5} \quad (2.30)$$

And we get the omega out of the spring constant by:

$$\omega = \sqrt{\frac{k}{m}} \quad (2.31)$$

So the resulting omegas are:

$$\omega_r = nIR^2d\sqrt{\frac{6\pi r^3\mu_0}{m(R^2 + d^2)^5}} \text{ and } \omega_z = 2nIR^2d\sqrt{\frac{6\pi r^3\mu_0}{m(R^2 + d^2)^5}} \quad (2.32)$$

Where r is the radius of the superconducting sphere.

We see that $\omega_z = 2\omega_r$. This means that the frequency peak for the translation z frequency is found at two times the frequencies in the x and y direction.

For the Lead Zeppelin with elliptical coils we can approximate the magnetic field as:

$$\vec{B}(x, y, z) = ax\hat{x} + by\hat{y} + cz\hat{z} \quad (2.33)$$

Where we need to compute a , b and c because the Taylor expansion is analytically hard to do.

Using the same approximations as in the thesis gives us the following force:

$$\begin{aligned} \vec{F}(x, y, z) = & -\frac{8\pi r^3}{3\mu_0}(a^2x\hat{x} + b^2y\hat{y} + c^2z\hat{z}) = \\ & -\frac{2V}{\mu_0}(a^2x\hat{x} + b^2y\hat{y} + c^2z\hat{z}) \end{aligned} \quad (2.34)$$

And the following frequencies:

$$\begin{aligned} \omega_x &= |a| \cdot \sqrt{\frac{2V}{\mu_0 m}} = |a| \sqrt{\frac{2}{\mu_0 \rho}} \\ \omega_y &= |b| \cdot \sqrt{\frac{2V}{\mu_0 m}} = |b| \sqrt{\frac{2}{\mu_0 \rho}} \\ \omega_z &= |c| \cdot \sqrt{\frac{2V}{\mu_0 m}} = |c| \sqrt{\frac{2}{\mu_0 \rho}} \end{aligned} \quad (2.35)$$

Where ρ is the density of lead.

2.2.4 Resonance Frequencies of a Cube

The easiest shape of superconductor to apply equation 2.28 to is a cube (that does not necessarily mean it is the easiest to solve). The cube has

edges with a length of $2l$ and its center at (x', y', z') . The faces are in the same plane as the Cartesian planes.

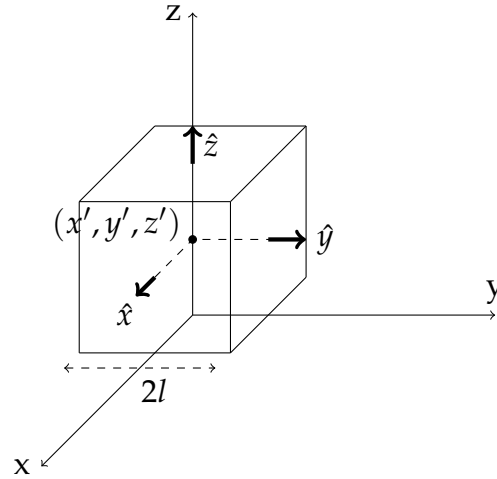


Figure 2.7: A cube in Cartesian coordinates.

We start by splitting the integral 2.28 in two parts:

$$\vec{F} = -\frac{2}{\mu_0} \left[\oint \vec{n} \|\vec{B}\|^2 dS - \oint \vec{B} (\vec{n} \cdot \vec{B}) dS \right] \quad (2.36)$$

For the magnetic fields we use the approximation from equation 2.33 again. The front and the back plane (with normal vector \hat{x} and $-\hat{x}$) are calculated first.

The first part becomes:

$$\begin{aligned} \oint \vec{n} \|\vec{B}\|^2 dS &= \oint \hat{x} (a^2 x^2 + b^2 y^2 + c^2 z^2) dS = \\ &= \int_{y=-l}^{y=l} \int_{z=-l}^{z=l} \left[a^2 (x' + l)^2 + b^2 y^2 + c^2 z^2 - a^2 (x' - l)^2 - b^2 y^2 - c^2 z^2 \right] \hat{x} dS = \\ &= \int_{y=-l}^{y=l} \int_{z=-l}^{z=l} 4a^2 x' l \hat{x} dS = 4a^2 x' l \cdot (2l)^2 \hat{x} = 16a^2 l^3 x' \hat{x} = 2Va^2 x' \hat{x} \end{aligned} \quad (2.37)$$

The second integral:

$$\begin{aligned}
 \oint \vec{B}(\vec{n} \cdot \vec{B}) \, dS &= \dots = \iiint B_x(\vec{\nabla} B_x) \, dV = \\
 \iiint a^2 x \hat{x} \, dV &= (2l)^2 \int_{x'-l}^{x'+l} a^2 x \hat{x} \, dx = \\
 2a^2 l^2 \hat{x} \cdot x^2 \Big|_{x'-l}^{x'+l} &= 8a^2 l^3 x' \hat{x} = Va^2 x' \hat{x}.
 \end{aligned} \tag{2.38}$$

A more detailed derivation can be found in the thesis of T. De Jong and D. Kok [12]

Combining both integrals gives the solution of the force in x direction:

$$F_x(x') = -\frac{2}{\mu_0}(2Va^2 x' - Va^2 x') = -\frac{2Va^2 x'}{\mu_0} \tag{2.39}$$

The total force will be:

$$\vec{F}(x, y, z) = -\frac{2V}{\mu_0}(a^2 x \hat{x} + b^2 y \hat{y} + c^2 z \hat{z}) \tag{2.40}$$

Which is exactly the same as equation 2.34, meaning that a superconducting sphere and cube both have the same frequencies.

We can also see that this is the same force acting on a superconducting block with different lengs l_1, l_2, l_3 . The integrand in the first integral is only a constant with a result depending only on the volume. In the second integral we can replace the limits with $x' + l_1$ and $x' - l_1$ and see that the result stays the same.

2.2.5 Mixing Frequencies

The force can be approximated linearly when it has a small deviation , but when we move further from the origin, other polynomials and crossterms

become important in the expansion. The complete expansion should look like:

$$\begin{aligned}
 F_x(x, y, z) = & -a_x x - a_{xx} x^2 - \dots - a_y y - a_{yy} y^2 - \dots - a_z z - a_{zz} z^2 - \dots \\
 & - a_{xy} xy - a_{xz} xz - a_{yz} yz - a_{xxy} x^2 y \dots = \\
 & - \sum_{n_x=0}^{\infty} \sum_{n_y=0}^{\infty} \sum_{n_z=0}^{\infty} a(n_x, n_y, n_z) x^{n_x} y^{n_y} z^{n_z}
 \end{aligned}
 \tag{2.41}$$

The solutions are not linear any more. This section and 2.2.6 are about these non-linearities.

In a Fourier spectrum we sometimes find the following frequencies as shown below:

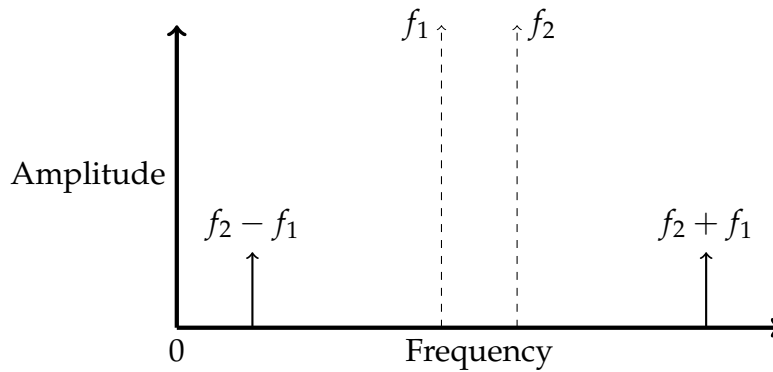


Figure 2.8: Two frequencies with their corresponding mixing frequencies.

The frequencies at $f_2 + f_1$ and $f_2 - f_1$ are called mixed frequencies and are caused by two signals multiplied together.

Let us assume two signals $x(t)$ and $y(t)$ with the condition $f_2 > f_1$:

$$x(t) = A \cos(2\pi f_1 t) \tag{2.42}$$

$$y(t) = B \cos(2\pi f_2 t). \tag{2.43}$$

The product of the two signals become:

$$x(t) \cdot y(t) = AB \cos(2\pi f_1 t) \cos(2\pi f_2 t). \tag{2.44}$$

For the Fourier Transform we can use a little trick called the "Convolution Theorem". This theorem states that the Fourier transform of a product is equal to the convolution of the Fourier transform of each component:

$$\mathcal{F}(x(t) \cdot y(t)) = \mathcal{F}(x(t)) \otimes \mathcal{F}(y(t)) \quad (2.45)$$

The convolution is an important tool in signal processing and is given by:

$$\boxed{X(f) \otimes Y(f) = \int_{-\infty}^{\infty} X(\tilde{f})Y(f - \tilde{f}) d\tilde{f}}. \quad (2.46)$$

Whereby the capital X is used from now on for the Fourier transform.

Anyhow, we still need to Fourier transform both signals apart, but this should be easy because the Fourier transform of a cosine is just two delta peaks.

$$\int_{-\infty}^{\infty} \cos(2\pi f_1 t) e^{-2\pi i f t} dt = \frac{1}{2} \left[\delta(f - f_1) + \delta(f + f_1) \right] \quad (2.47)$$

The Fourier Transform of both signals then become:

$$X(f) = A \int_{-\infty}^{\infty} \cos(2\pi f_1 t) e^{-2\pi i f t} dt = \frac{A}{2} \left[\delta(f - f_1) + \delta(f + f_1) \right] \quad (2.48)$$

$$Y(f) = B \int_{-\infty}^{\infty} \cos(2\pi f_2 t) e^{-2\pi i f t} dt = \frac{B}{2} \left[\delta(f - f_2) + \delta(f + f_2) \right]. \quad (2.49)$$

Putting this in the convolution integral 2.46 gives:

$$X(f) \otimes Y(f) = \frac{AB}{4} \int_{-\infty}^{\infty} \left[\delta(\tilde{f} - f_1) + \delta(\tilde{f} + f_1) \right] \left[\delta(f - f_2 - \tilde{f}) + \delta(f + f_2 - \tilde{f}) \right] d\tilde{f}. \quad (2.50)$$

We can split this integral into two parts:

$$\frac{AB}{4} \int_{-\infty}^{\infty} \left[\delta(\tilde{f} - f_1) + \delta(\tilde{f} + f_1) \right] \delta(f - f_2 - \tilde{f}) d\tilde{f} \quad (2.51)$$

$$+ \frac{AB}{4} \int_{-\infty}^{\infty} \left[\delta(\tilde{f} - f_1) + \delta(\tilde{f} + f_1) \right] \delta(f + f_2 - \tilde{f}) d\tilde{f}. \quad (2.52)$$

Using the property of the Dirac-delta:

$$\int_{-\infty}^{\infty} X(\tilde{f}) \delta(f - \tilde{f}) d\tilde{f} = X(f), \quad (2.53)$$

the answer to the whole Fourier Transform becomes:

$$\frac{AB}{4} \left[\delta(f - f_1 - f_2) + \delta(f + f_1 - f_2) + \delta(f - f_1 + f_2) + \delta(f + f_1 + f_2) \right]. \quad (2.54)$$

We only want to look at the positive frequencies. We also stated that $f_2 > f_1$, so the only interesting part then becomes $\delta(f - f_1 - f_2) + \delta(f + f_1 - f_2)$. This says that two peaks will be shown, one at $f_2 + f_1$ and one at $f_2 - f_1$.

2.2.6 Double Frequencies

In the Fourier Spectrum of the spherical Lead Zeppelin with the circular coils we also find double frequencies. We think that these arise from the back action of the connected coils.

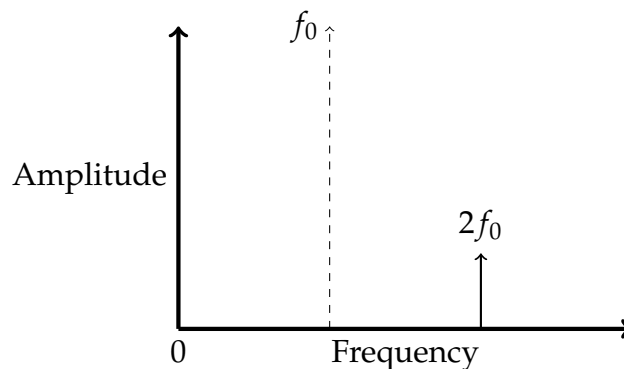


Figure 2.9: A frequency with its corresponding double frequency.

Double frequencies are caused by the signal squared. The procedure of getting the Fourier transform is almost the same as above so some parts will be shortened.

We start with one signal

$$x(t) = A \cos(2\pi f_0 t) \quad (2.55)$$

And multiply it with itself

$$x(t)^2 = A^2 \cos^2(2\pi f_0 t) \quad (2.56)$$

We will use the convolution theorem 2.45 again but now with the signal itself

$$\mathcal{F}(x(t)^2) = X(f) \otimes X(f) \quad (2.57)$$

By using the Fourier transform of a cosine, which was given in 2.47, we can find the answer to the convolution integral.

$$\begin{aligned} & \frac{A^2}{4} \int_{-\infty}^{\infty} \left[\delta(\tilde{f} - f_0) + \delta(\tilde{f} + f_0) \right] \left[\delta(f - f_0 - \tilde{f}) + \delta(f + f_0 - \tilde{f}) \right] d\tilde{f} = \\ & \frac{A^2}{4} \left[\delta(\tilde{f} - 2f_0) + \delta(f) + \delta(f) + \delta(f + 2f_0) \right] = \\ & \frac{A^2}{4} \left[2\delta(f) + \delta(f - 2f_0) + \delta(f + 2f_0) \right] \end{aligned} \quad (2.58)$$

The $\delta(f - 2f_0)$ indicates that it shows a peak at $2f_0$.

Materials and Methods

3.1 The Circuit

3.1.1 The Scheme

The circuit being used for this experiment is shown in figure 3.1. Almost all the wires are type II superconducting niobium-titanium, which are stronger wires than niobium so easier to work with. Only the shortcut running through the big coil is niobium.

The number correspond to the following sources and meters:

- 1 - Voltage meter.
- 2 - Current source.
- 3 - Voltage source for the big coil.
- 4 - An extra pair of wires which can be used for improvements later, therefore not visible in the figure.
- 5 - Function generator.

The dashed box is the switch with the shortcut running through. The essence of this switch will be explained in the next subsection. The current source provides a current through the shortcut and elliptical coils. The voltage meter measures the voltage over this part. In between the two elliptical coils we see a pick-up loop connected to a SQUID. This loop picks up the flux running through and the SQUID, a sensitive magnetometer, converts it to data. The excitation loop is connected to a function generator and can drive the lead particle. Finally, the Zeppelin can be seen in

between.

The part of the circuit which stays at room temperature is in the pink box. The part which goes in the barrel of helium at 4.2 Kelvin, is given in the blue box.

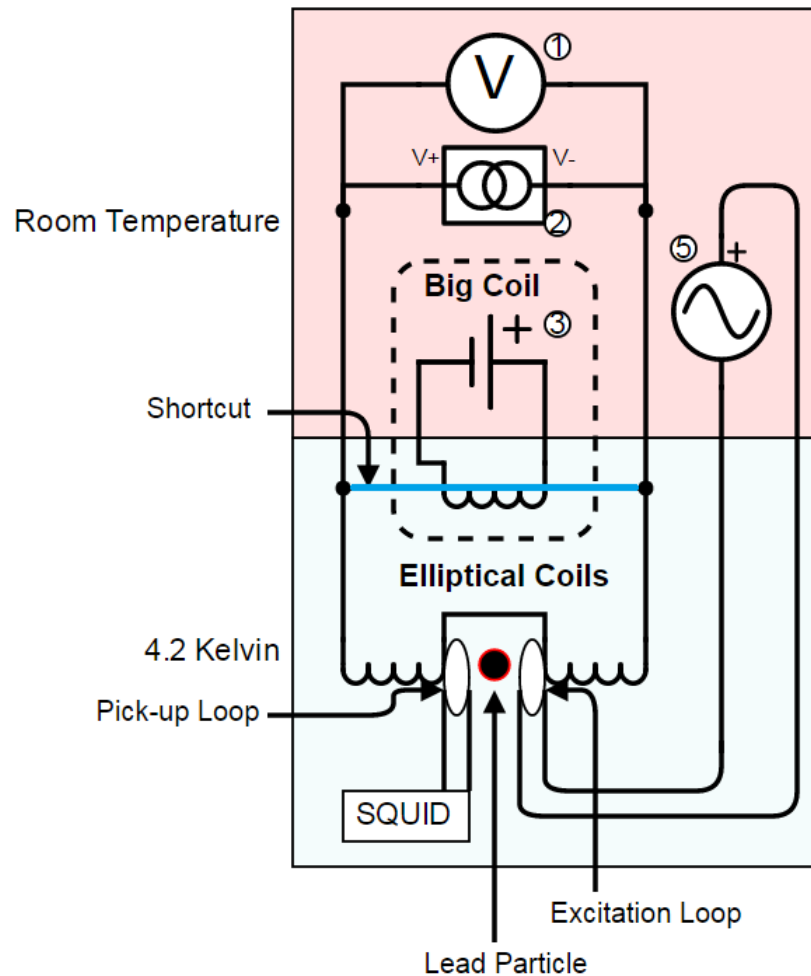


Figure 3.1: The circuit used in the project.

3.1.2 The Switch

We want to enforce a steady current through the elliptical coils. However, when we connect the current source directly to the elliptical coils, the coils will pick up the noise from the current source and the wires outside the coils. Therefore it would be better to have a current flow only through loop

of the coils with the source cut off. This loop can be seen in the blue part of figure 3.1 and consists of the elliptical coils and the blue wire through the big coil.

The switch consists of a big coil which can reach a magnetic field above the critical magnetic field of the niobium wire running through.

The shortcut and elliptical coils are parallel connected, so they both receive the same voltage.

$$V = I_R R = -L \frac{dI_L}{dt} \quad (3.1)$$

Where R is the resistance of the shortcut wire and L the inductance of both coils. This is a first order differential equation so the solution for the current through the coils, with condition $I_L(0) = 0$, is:

$$I_L = I_T (1 - e^{-\frac{R}{L}t}) \quad (3.2)$$

With I_T as total current $I_T = I_R + I_L$.

When the switch is turned off, the resistance R through the shortcut is zero. This means that $I_L = 0$ and all the current will run through the shortcut. When the switch is turned on, the shortcut will become a wire with a normal resistance and we can see a charge build-up in the elliptical coils.

We can first let the charge build up in the elliptical coils. When they are almost loaded and have enough electrical energy, we can turn off the switch. Because the wires running back to the source have a higher resistance, the energy built up in the coils will release through the zero resistance shortcut. This results in an independent current through the RL-circuit, thus the current source can be turned off.

For this to happen, we have to be sure that the magnetic field created by the big coil is higher than the critical field of niobium. The critical field for niobium to become normal conducting is at 400 mT in vacuum. The on-axis magnetic field of a solenoid is calculated in Martin's thesis "The Lead Zeppelin Project" [4]:

$$B = \frac{n\mu_0 I}{2r} \quad (3.3)$$

For r the middle between the outer and inner radius of the coil can be chosen. A quick estimation with constants: $I = 0.5\text{A}$, $r = 8\text{mm}$, $B = 400\text{mT}$ gives $n \approx 10^4$.

One may see that the coils are connected in series. This is because the moving lead particle induces an electromotive forces in the coils which changes the magnetic field. To keep the field constant, it is connected in series so every induced electromotive force in one coil is equally given to the other coil to keep the sum of the forces zero.

3.1.3 Twisting Wires

To keep the incoming flux as minimum as possible, the wires are twisted (see section 2.1.1). Some wires can only be twisted by hand but for long wires there is a little trick. Start by cutting off a wire twice as long. Put equal weights on both ends of the wire.



Figure 3.2: The weights used for the ends

Determine the middle of this wire and hang it from somewhere high. One

weight should just be above the other. Twist the top part of the wire and the weights will start to follow in a circular motion. After some twists, the weights have gained a momentum and the wire will start twisting on its own. The reason for having the weights not on the same height is that they will keep spinning longer in the end.

When the wires are done spinning, glue can be applied to the whole wire to make it stronger. Do not take the wire off immediately, try to keep it as straight as possible. When the tension on the wire releases, curls will sometimes occur like the figure below.



Figure 3.3: *The telephone curl effect on a wire.*

Hold the big loop of the curl and twist it in the other direction until it does not appear any more. It is important not to pull the wire straight because after the curls have formed, they will cause sharp bends in the wire which can affect the conductivity. The bends will also cause trouble when inserting the wires in a teflon sock, which offers protection from breaking the wires when pulled.

3.2 The Elliptical Coils

3.2.1 Winding the Coils

In the circuit we see two opposite placed coils which are connected in serie. The blueprint for one holder of the coils is shown below in figure 3.4. These holders are made of plastic.

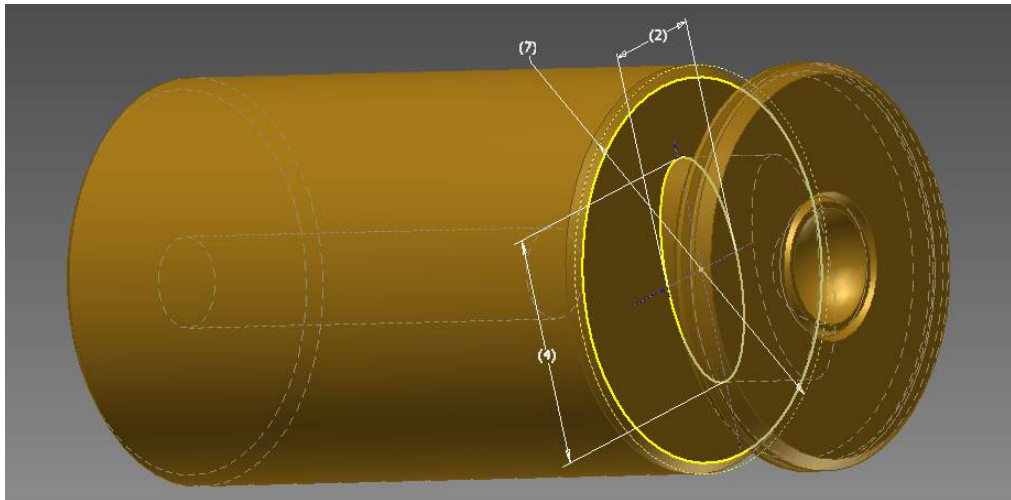


Figure 3.4: A holder

We see that the elliptical base has a diameter of 4 mm and 2 mm, a niobium-titanium wire is wounded up 255 times around this part. The diameter of the whole coil is 7 mm. The dimensions of the length do not really matter. There is a cave at the top where we can trap the lead particle when the two coils are placed against each other. Around this cave we see a groove where the pick-up loop can be placed. The groove leads to the outside, which is not shown in the picture. The wire is made of niobium and picks up the flux of the field. This wire eventually leads back to the SQUID. Furthermore, we see a slit around the top where we will glue in a excitation loop which can give a driving force on the lead particle. We only need one pick-up loop and one excitation loop so we can give one coil the pick-up loop while the other one has the excitation loop. This way we make sure that they will be less in each others way.

The windings are made by placing the holder in a rotating device as seen in figure 3.5 which can be spun by a motor or by hand. Spinning by hand gives more control but requires more effort. Winding the coil becomes easier when a microscope is used.



Figure 3.5: The holder in the rotating device. One end of the wire is taped to the rotator and the other is held with tension from the wire coil.

The coil where the niobium-titanium wire comes from should be able to freely rotate without much resistance and should be mounted in a place where the wire to the holder does not become obstructed.

The wire is rolled out to the holder. Around 10 cm from the beginning of the wire, a part is glued to the corner which is closest to the long part of the holder, the left corner in figure 3.5. We can rotate the device, but it is important to remember which way the rotating occurs because the second holder should also be rotated in the same direction. The wires should be as tight as possible. A needle can be used but be aware that the sharp point does not scrape the coating of the wire. After a few windings, some glue can be applied on top to make sure the wire stays in place. This is repeated until the coil has 255 windings. The wire should come out at the left corner and be cut off at length of around 10 cm. These two wires

should be twisted together. The process for the second coil is exactly the same.

One coil has the pick-up loop while the other gets the excitation loop. Winding the excitation loop is just a case of fitting a niobium-titanium wire around the top and glueing, leaving ends of 10 cm. The pick-up loop requires more work: it is made of more fragile 50 μm niobium wire and winded around the smaller loop around the cave. The excitation loop wires needs to be twisted with itself and the pick-up loop wire also with itself.

Finally, a layer of phenol is applied to keep the coil really firm.

If a small mistake occurs, the glue can be dissolved using acetone. The remaining glue could be scraped off with the needle. If there is still too much glue, the holder can be placed in a beaker with acetone and shaken thoroughly.

3.2.2 Assembling the Coils

The two coils are assembled in a special case as seen below in figure 3.6. We can neglect the green part. It is necessary that the long side of the ellipses are placed along the same direction without any deviation. The grooves where the pick-up loop comes out can be seen from the outside. These grooves both run out at the long side of the coils and can therefore be used to calibrate the ellipses. The grooves should be on top of each other.

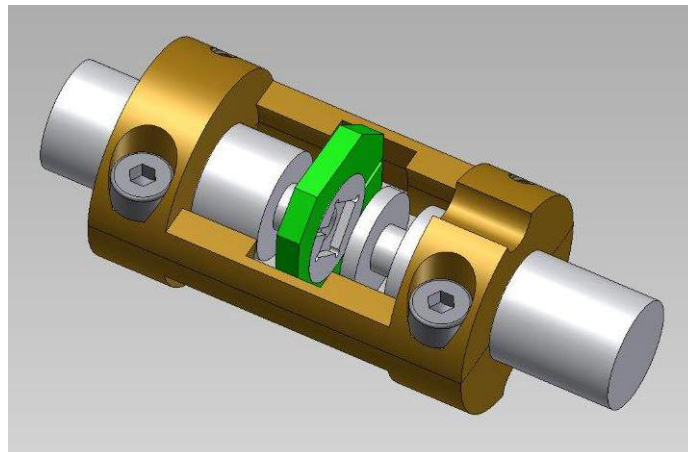


Figure 3.6: The assembly for the coils.

In figure 3.6 we can see a circular cut out part at the right side of the assembly. A similar cut can be seen on the other side on the right of the assembly. The niobium-titanium wires should run along one cut and the niobium pick-up wire along the other cut.

The whole assembly is placed in a niobium container with the wires running out as seen in figure 3.7.

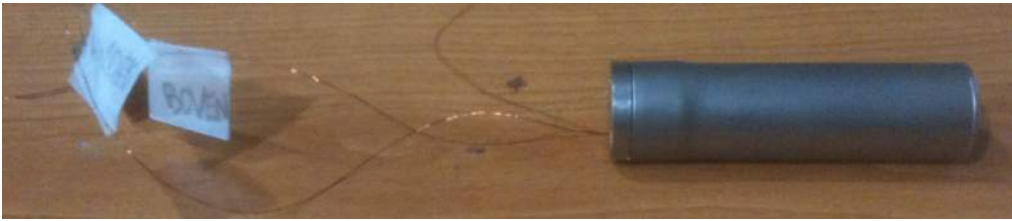


Figure 3.7: The metal container with the wires running out marked "Boven" and "Onder".

The superconducting Nb container encloses a Faraday cage and keeps the assembly free from EM noise.

3.3 The Big Coil

3.3.1 The Machine

A machine (figure 3.8) is used for winding the big coil. This is because the big coil requires a lot more windings: around 10.000. This was calculated with equation 3.3.



Figure 3.8

The machine consists of:

A wire coil

This is the white coil on top where the niobium-titanium wire runs off. Be sure that it still has enough wire: the big coil needs around 500 m!

The big coil

The big coil is the coil in the middle of the figure where the light shines upon and is made of plastic.

The dimensions of the big coil are:

length = 18mm, inner radius = 4.5mm and the outer radius = 11mm. The big coil also has a hole for the shortcut to run through which has a radius of 1.5mm. The dimensions are chosen such that with wire of a diameter of $120\mu\text{m}$, $n = 8125$ can be reached.

A leading wheel

The wire from the wire coil runs through a leading wheel, which goes back and forth to spin the wire evenly over the big coil. The leading wheel can be seen just above the big coil. The back and forth motion of the leading wheel can be turned off on the machine. The velocity at which it goes is determined by setting the diameter of the wire. The boundaries at which it goes back and forth is limited by adjustable locks on each side.

A microscope

The microscope can be seen on the left side and is directed at the big coil.

A counter

The counter is on the left side of the green machine and gives the count in numbers. Be sure to set the counter to zero when you start with wiring. In this case, the counter gives one count every two windings so the value must be doubled to get the true number of windings.

A pedal

The pedal is on the ground and turns on the rotating device. The velocity depends on how far the pedal is pushed in. The maximum velocity is adjustable on the machine.

3.3.2 Making the Big Coil

Locking something in the rotating device works the same as locking a drill bit into a drill machine. So a drill bit has to be found which can fit in the hole of the big coil. To make it tight, we can use teflon tape around the drill bit.

Start with a segment glued to the side of the coil away from the drill. Tape the rest of the wire to the outside radius of the big coil. The reason for not taping the wire to the other side is because the wire can break when the machine keeps spinning but the big coil stops, which occurred in several

cases.

Try to keep everything as tight as possible, especially the sides. After a while this becomes impossible but how tighter it is in the beginning, how easier the rest of the winding becomes.

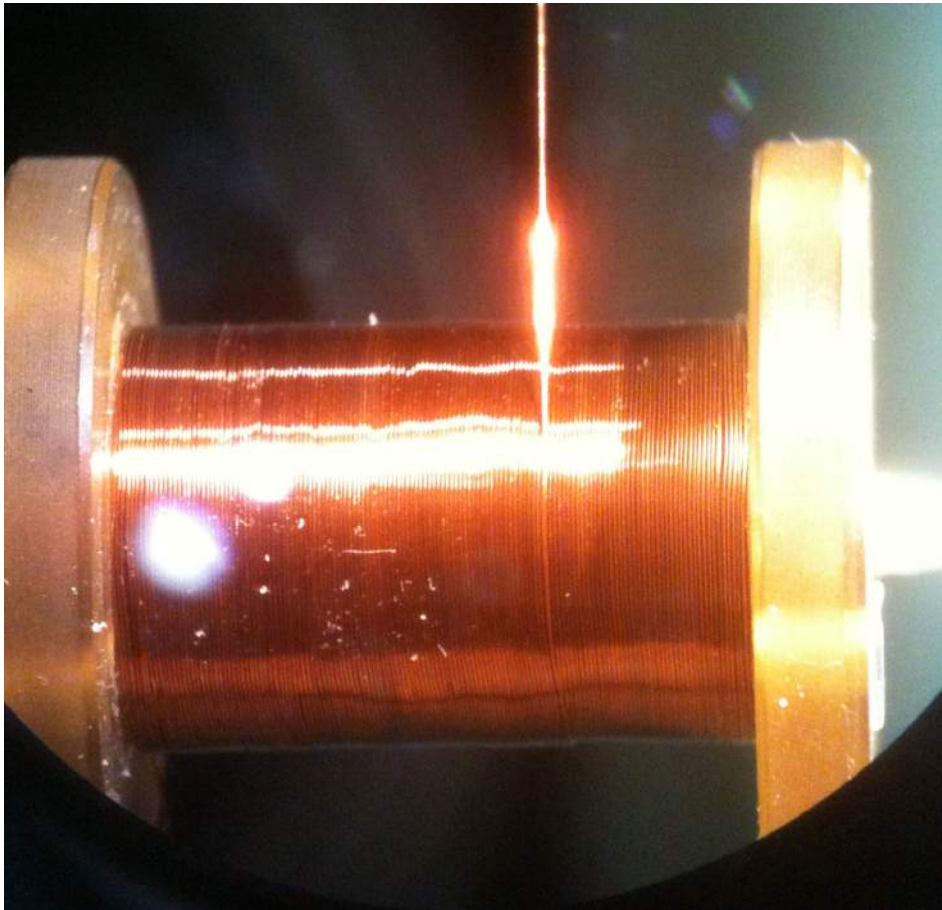


Figure 3.9: A picture of the big coil taken to the microscope, hence the black circle on the bottom. Note how tightly the wire is stuck together.

A way to keep it tight is to let the leading wheel run a bit behind the position of the wire on the coil and have some tension on the wire. The tension causes the wire to fall tightly to the side of the winding before. Glue can be applied every once in a while to keep it in place, but the downside in this case is that the wire becomes harder to use when everything needs to be done again.

In this experiment the wire ran out at 6828 windings. We can look at the current needed to provide a field higher than the critical field of niobium.

Equation 3.3 rewritten gives:

$$I = \frac{2B_{crit}r}{\mu_0 n} \approx 0.723A. \quad (3.4)$$

This is quite a high current, and can result in the experiment heating up. Experiments have to be made to make sure that this does not happen.

A layer of Stycast is put over the wires to make it stable. The Stycast needs a day to dry at room temperature. This process can be accelerated using a blow-dryer.

The ending of both wires should also be twisted and put in a teflon sock. This sock should then be hold on one side of the big coil with a thread. Let the big coil stand on the other side and apply a layer of Stycast over the side with the teflon sock. Be careful that no Stycast comes into the hole where the niobium wire goes through, we can close this hole off with a cotton bud. The same procedure is done on the other side.

Put the coil back on the machine and let it run at a low velocity with a big layer of Stycast all around it. This amount of Stycast is necessary to make sure the coil does not explode when it reaches a temperature of 4 Kelvin.

The big coil now looks like a black barrel with a clear hole in the middle and a teflon sock with wires running out of it.



Figure 3.10: The final product of the big coil

3.4 The Lead Particles

The lead particles are made by scraping off a little bit from a bigger block of lead. Gloves can be worn to protect against lead dust on the hands. The scraped off lead is put on a thick piece of metal. This metal will become really hot so it must be placed well. With the help of a Dremel burner we heated up the lead scrape until it starts to melt a bit. The burner should not heat the scrape too long, there must be small pauses between every heating.



Figure 3.11: The Dremel burner

The scrape melts faster when it is occasionally turned around. Eventually the scrape will turn into a round ball.

In this experiment five balls are made: 2 small sized and 3 large sized as can be seen in figure 3.12.



0.5mm

Figure 3.12: The balls seen under a microscope.

The wire running underneath the balls is a 50 μm niobium wire. The diameter, and therefore the mass can be approximated with the picture. We look at how many times the wire fit in the balls by zooming in the picture.

The volume is calculated by $V = \frac{4}{3}\pi r^3 = \frac{1}{6}\pi d^3$.

The mass is calculated by $m = \rho V$ where $\rho = 11.34 \text{ g/cm}^3$.

	n times width wire	d (cm)	V (cm ³)	m (g)
small balls	4.5	$2.25 \cdot 10^{-2}$	$5.96 \cdot 10^{-6}$	$6.76 \cdot 10^{-5}$
large balls	6	$3.00 \cdot 10^{-2}$	$1.41 \cdot 10^{-5}$	$1.60 \cdot 10^{-4}$

The balls are given different shapes with the help of pliers until they look like the figure below.

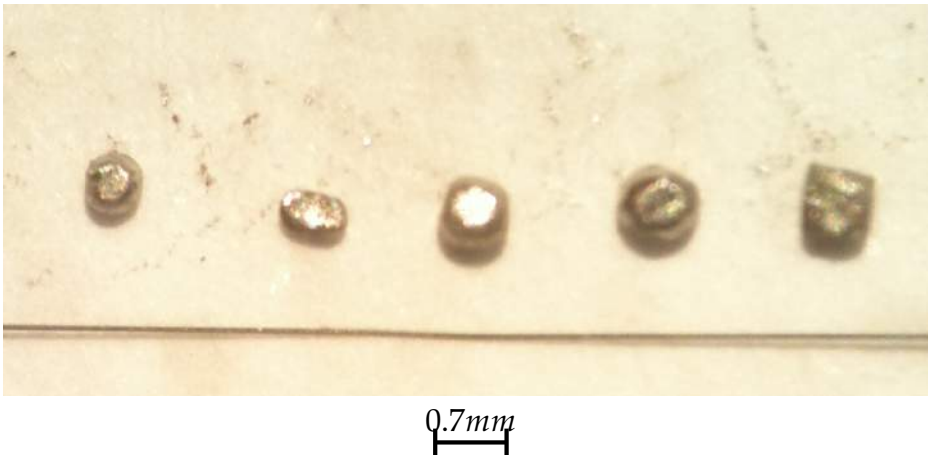


Figure 3.13: The balls after giving dents

From left to right they got the shape by:

2 light dents - 2 hard dents - 2 light dents - 3 light dents - 3 hard dents.

3.5 Preparing the Dipstick

The dipstick is a long stick with a plate on the end where the experiment will be mounted. The stick goes in a barrel with helium-4 where it will reach a temperature of 4 Kelvin, therefore below the critical temperature of niobium-titanium, niobium and lead.

We begin by making two cables which send data back and forth through the stick. One cable is for the SQUID and connects to a 14 pins female LEMO on the top, the other cable ensures data flow from the coils and connects to a 24 pins Fischer.

Below we see the 24-pins Fischer with the corresponding data numbers. We want to solder 10 niobium-titanium wires to the numbers 1 to 10 but it becomes easier if we prepare the wires first.



Figure 3.14: 24 pins Fischer LEMO

One wire with a length a bit longer than double the dipstick is twisted with the method used in section 3.1.3. The wire is cut in the middle so it becomes two wires. Enter these two wires through a teflon sock. Any bends will make it harder for the wire to be entered through the sock.

Another way to get them through is by soldering a stronger wire to the two wires and running this wire first through the sock. The two wires can then be pulled through when the stronger wire is starting to exit.

We end with five teflon pairs. The pairs are labeled 1 to 5 with the label close to one end.

Solder the wires with the label '1' to the pockets 1 and 2, label '2' to pockets 3 and 4 etc. The labels need to be close to the other end of the wires.

We make sure they conduct by measuring the resistance. The ten wires are run through a metal coating to ensure a Faraday cage. The coating has the same length as the tube of the dipstick, but because the wires are longer, the wires will stick out with the labels on this end. To ensure stability, we put a layer of Stycast around the coating where it makes contact with the Fischer. We put silver coating around this to close the Faraday cage.

The second cable can be bought to fit from the SQUID to a 14-pins LEMO.

Run these two cables first through the dipstick so they end at the plate. The labels need to be visible here.

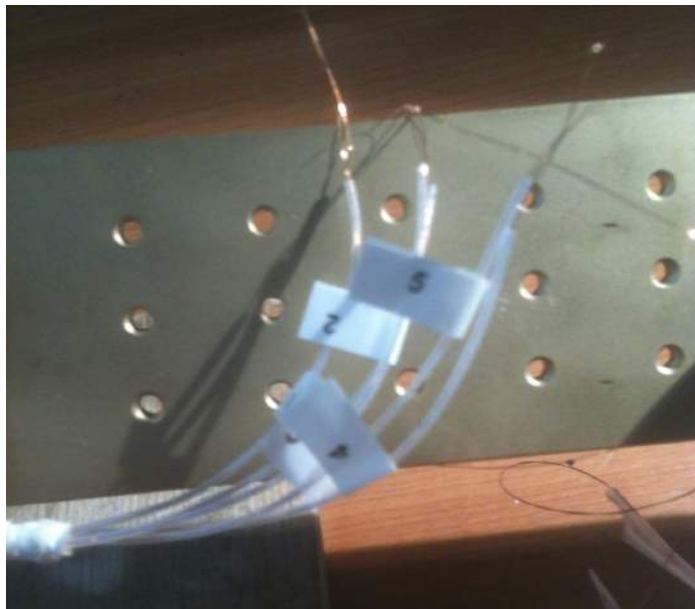


Figure 3.15: The wires with their corresponding labels.

We then mount the elliptical coils on the plate with a special design with screws the tube to the plate.



Figure 3.16: *The wires are not in this picture because we did it the other way around and ended up taking apart everything because one cable did not fit through.*

The wire which runs from the pickup coil in between the elliptical coils to the SQUID needs to be put in a teflon sock first, and then through a lead tube which fits tightly around the sock. To cut the lead tube, be sure to have a thicker wire running through so the pressure will not close the ends together.

We can put the squid on the plate to see where it fits.



Figure 3.17: *The elliptical coils are put some notches back to make room for the SQUID.*

The big coil is put on this plate next to the SQUID and held using teflon tape.

Everything is spot welded together using niobium as the connector between the wires and Kapton tape around to ensure everything stays in place. The labels correspond to the numbers in the scheme (figure 3.1).

The wire which goes through the big coil is spot welded as seen in the circuit (figure 3.1). This wire is bend in the middle and twisted. After this it is then put through the big coil. This way we can easily remove the wire if there occur any problems.

The SQUID cable is fit into the SQUID. Layers of teflon tape are wound up around the plate until everything stays tightly together.



Figure 3.18: The experiment taped together with teflon tape. This way everything stays tight together.

The last thing to do is to slip a cone around the plate, this way we can suck the experiment until it creates a vacuum. Some high-vacuum grease must be applied at the point where it makes contact with the cone. The end product is shown in figure 3.19.



Figure 3.19: *The final product of the dipstick.*

The only work to do on the other side is to assemble a manometer.

Chapter 4

Numerical Calculations and Predictions

4.1 The Magnetic Field

The codes are written in Mathematica. They are meant for the elliptical coils, but can be used for the circular coils when a and b are made equal. The equations for the magnetic field are exactly the same as 2.22, 2.23 and 2.24.

The constants we use are close to the correct constants of the experiment.

```
mu0 = 4*Pi*10(-7) (*The magnetic permeability of air*);  
  
i = 0.25 (*The current in Ampere*);  
a = 2 (*Distance between origin and ellipse along x in mm*);  
b = 1 (*Distance between origin and ellipse along y in mm*);  
d = 1 (*Distance between the origin of the ellipse and z=0 in mm*);  
n = 255 (*Number of windings*);
```

The reason why millimeters are used instead of the SI-Unit "meter" is because Mathematica gives much better streamplots when higher numbers are used.

The code for the magnetic field of two elliptical coils in an AH-configuration are given below. We use NIntegrate instead of Integrate because Integrate tends to calculate the integration in mathematical form while NIntegrate

calculates everything numerically, and is therefore quicker.

```

bx[x_?NumericQ, y_?NumericQ, z_?NumericQ] :=
mu0*i*b*n/(4*Pi)*
  NIntegrate[((z +
    d)/(x^2 + y^2 + (z + d)^2 + a^2*Cos[t]^2 + b^2*Sin[t]^2 -
    2*a*x*Cos[t] - 2*b*y*Sin[t])^(3/2) - (z -
    d)/(x^2 + y^2 + (z - d)^2 + a^2*Cos[t]^2 + b^2*Sin[t]^2 -
    2*a*x*Cos[t] - 2*b*y*Sin[t])^(3/2)) Cos[t], {t, 0, 2 Pi}]
  (*The x component of the magnetic field*)

by[x_?NumericQ, y_?NumericQ, z_?NumericQ] :=
mu0*i*b*n/(4*Pi)*
  NIntegrate[((z +
    d)/(x^2 + y^2 + (z + d)^2 + a^2*Cos[t]^2 + b^2*Sin[t]^2 -
    2*a*x*Cos[t] - 2*b*y*Sin[t])^(3/2) - (z -
    d)/(x^2 + y^2 + (z - d)^2 + a^2*Cos[t]^2 + b^2*Sin[t]^2 -
    2*a*x*Cos[t] - 2*b*y*Sin[t])^(3/2)) Sin[t], {t, 0, 2 Pi}]
  (*The y component of the magnetic field*)

bz[x_?NumericQ, y_?NumericQ, z_?NumericQ] :=
mu0*i*n/(4*Pi)*
  NIntegrate[(1/(x^2 + y^2 + (z + d)^2 + a^2*Cos[t]^2 +
    b^2*Sin[t]^2 -
    2*a*x*Cos[t] - 2*b*y*Sin[t])^(3/2) -
    1/(x^2 + y^2 + (z - d)^2 + a^2*Cos[t]^2 + b^2*Sin[t]^2 -
    2*a*x*Cos[t] - 2*b*y*Sin[t])^(3/2)) (a*b - a*y*Sin[t] -
    b*x*Cos[t]), {t, 0, 2 Pi}] (*The z component of the magnetic
    field*)

```

It would be nice to look at the symmetric properties of the elliptical fields. We can therefore plot the field in a $y=0$ and $x=0$ plane.

```
StreamPlot[{bx[x, 0, z], bz[x, 0, z]}, {x, -3, 3}, {z, -3, 3},
  StreamColorFunction -> "Rainbow",
  PlotLabel -> "Magnetic Field Lines",
  FrameLabel -> {"x(mm)", "z(mm)"},
  PlotLegends ->
  BarLegend[Automatic,
    LegendLabel -> "Magnetic Field Intensity (kT)"] (*Streamplot in
    y=0 plane*)
```

```
StreamPlot[{by[0, y, z], bz[0, y, z]}, {y, -3, 3}, {z, -3, 3},
  StreamColorFunction -> "Rainbow",
  PlotLabel -> "Magnetic Field Lines",
  FrameLabel -> {"y(mm)", "z(mm)"},
  PlotLegends ->
  BarLegend[Automatic,
    LegendLabel -> "Magnetic Field Intensity (kT)"] (*Streamplot in
    x=0 plane*)
```

This code gives the figures 4.1(a) and 4.1(b).

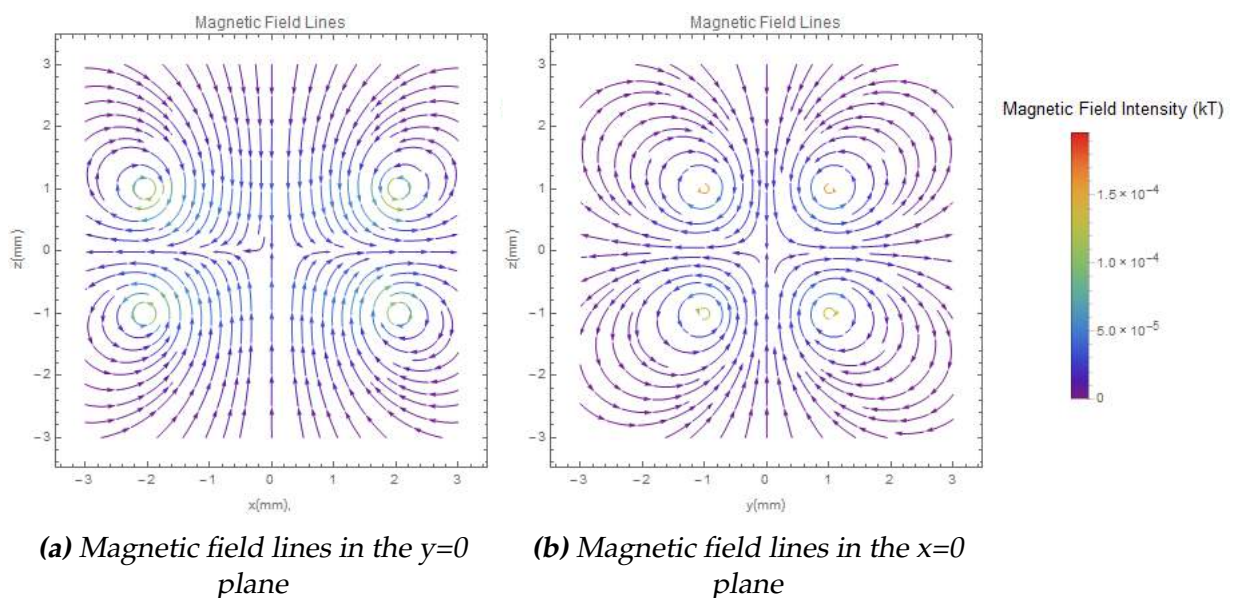


Figure 4.1

We can clearly see the radii¹ of the current loop. In the $y=0$ plane the upper current loop shows a radius of 2 and in the $x=0$ plane a radius of 1. Because we work in millimeters, the unit of the magnetic field is in kT.

The graphs show some problems: anti-symmetry around $(0,0)$ in both figures 4.1(a) and 4.1(b). This is probably because of the way how Mathematica calculates the streams. The way the upper half of the function interacts with the lower half around $(0,0)$ can force Mathematica to take arbitrary values. We can look if this is true by plotting with different limits.

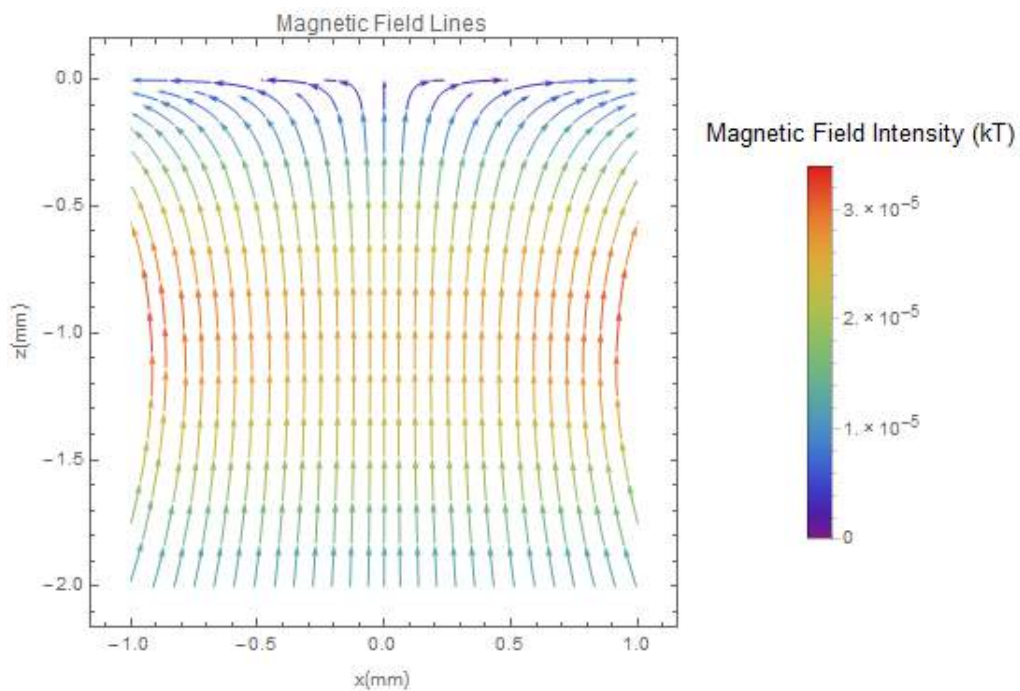


Figure 4.2: The limits are changed: $x = \{-1, 1\}$ and $z = \{-2, 0\}$

We see that the function is now symmetric and the anti-symmetry is caused by Mathematica.

¹The meaning of the radius of an ellipse can differ. In this case we mean the distance a and b.

To see the elliptical field in the $z=0$ plane clearly, we can make a vectorplot.

```
VectorPlot[{bx[x, y, 0], by[x, y, 0]}, {x, -3, 3}, {y, -3, 3},
  VectorColorFunction -> "Rainbow",
  PlotLabel -> "Magnetic Field Vectors",
  FrameLabel -> {"x(mm)", "y(mm)"},
  PlotLegends ->
  BarLegend[Automatic, LegendLabel -> "Field Intensity (kT)"]
  (*Vector plot in the z=0 plane*)]
```

With its corresponding figure:

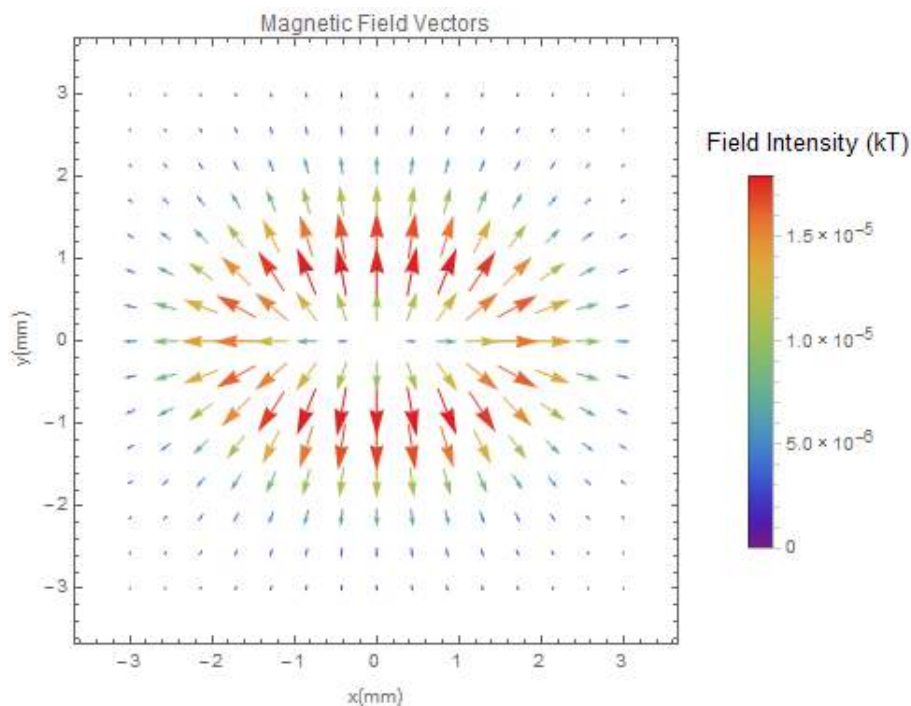


Figure 4.3: The largest vectors are close to the shape of the elliptical coils

We see that in the middle it has no magnetic field. This is a property of the anti-Helmholtz configuration. The potential is lowest at this point so the particles tend to stay as close as possible to this point.

A 3D Plot can also be made of the magnetic field. Unfortunately, there is no 3D streamplot function in Mathematica. We can use a 3D vector plot but this function scales the vectors to the vector with the highest value. If we look at figure 4.3 we see that it has large red vectors around the ellipse

and small vectors on the side of the graph. The big difference between values of the vectors causes the 3D plot to act chaotically.

Also, the experiment takes place around the origin. So for the 3D plot it is better to take values limits close to the origin.

```

VectorPlot3D[{bx[x, y, z], by[x, y, z], bz[x, y, z]}, {x, -0.8,
  0.8}, {y, -0.8, 0.8}, {z, -0.8, 0.8},
VectorColorFunction -> "BlueGreenYellow",
PlotLabel -> "Magnetic Field Vectors",
AxesLabel -> {"x(mm)", "y(mm)", "z(mm)"},
PlotLegends ->
  BarLegend[Automatic, LegendLabel -> "Field Intensity (kT)"] (*3D
  Vector plot*)

```

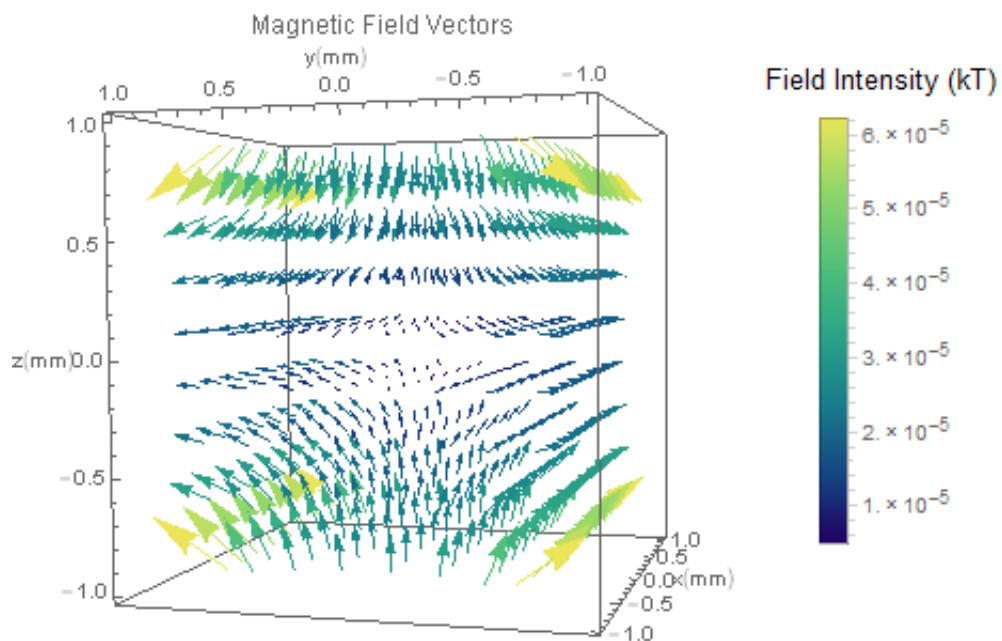


Figure 4.4: A three dimensional plot of the field close to its zero potential.

In the 3D plot we see how the magnetic fields build up around the origin. How further we go, how intenser the magnetic field gets.

4.2 Approximating the Magnetic Field

The constants are converted to SI-units so the magnetic field is calculated in Tesla. This is convenient because the magnetic field is going to be numerically approximated.

```
mu0 = 4*Pi*10^(-7) (*The magnetic permeability of air*);

i = 0.25 (*The current in Ampere*);
a = 2*10^-3 (*Distance between origin and ellipse along x in m*);
b = 10^-3 (*Distance between origin and ellipse along y in m*);
d = 10^-3 (*Distance between the origin of the ellipse and z=0 in
           m*);
n = 255 (*Number of windings*);

ds = 10^-5 (*The infinitesimal length for the derivatives*);
```

The code for the plots of the magnetic fields is shown below.

```
Plot[bx[x, 0, 0], {x, -10^-3, 10^-3},
     PlotLabel -> "Value Magnetic Field", AxesLabel -> {"x(m)",
               "Bx(T)"}] (*The x-component of the magnetic field*)

Plot[by[0, y, 0], {y, -10^-3, 10^-3},
     PlotLabel -> "Value Magnetic Field", AxesLabel -> {"y(m)",
               "By(T)"}] (*The y-component of the magnetic field*)

Plot[bz[0, 0, z], {z, -10^-3, 10^-3},
     PlotLabel -> "Value Magnetic Field", AxesLabel -> {"z(m)",
               "Bz(T)"}] (*The z-component of the magnetic field*)
```

This code creates three plots with the components of the magnetic field to their corresponding directions. These are the plots needed to look at the linearities of the field around the origin. If they are linear enough, we can safely calculate the polynomial constants. The plots of the code are shown below:

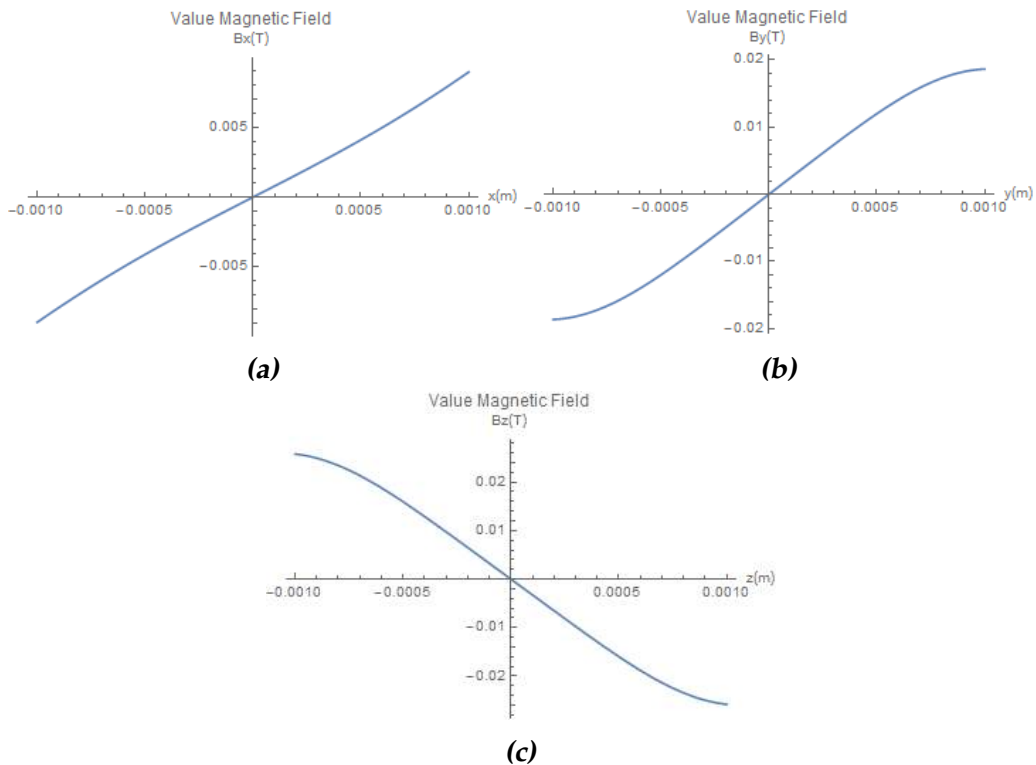


Figure 4.5: The magnetic fields with the same limits as the sphere in which the Zeppelin can move.

At the edges we can see the slope decreasing which indicates a third degree polynomial. However, for the following calculations we assume that the particle stays close to the origin and can therefore be approximated with a first degree polynomial as shown in equation 2.33).

These constants are found by taking the derivative of the function at their origins. The derivative is calculated by:

```

a1 := (bx[ds, 0, 0] - bx[-ds, 0, 0]) / (2 *
      ds) (*The derivative of bx to x*)
b1 := (by[0, ds, 0] - by[0, -ds, 0]) / (2 *
      ds) (*The derivative of by to y*)
c1 := (bz[0, 0, ds] - bz[0, 0, -ds]) / (2 *
      ds) (*The derivative of bz to z*)

```

The 1 indicates the slope constants, because a and b are already defined for the elliptical properties.

And gives the following slopes:

```
In[228] := {a1, b1, c1}
```

```
Out[228] = {7.90315, 24.6639, -32.567}
```

The resulting magnetic field will then be:

$$\vec{B}(x, y, z) = 7.90x\hat{x} + 24.66y\hat{y} - 32.567z\hat{z}. \quad (4.1)$$

Remarkable is how the absolute of the slope in the z direction is the sum of the other two slopes. This is explained by one of the Maxwell's equations, namely:

$$\vec{\nabla} \cdot \vec{B} = 0 \quad (4.2)$$

Which gives:

$$\frac{\partial}{\partial x}a_1x + \frac{\partial}{\partial y}b_1y + \frac{\partial}{\partial z}c_1z = a_1 + b_1 + c_1 = 0 \quad (4.3)$$

4.3 Resonance Frequencies

4.3.1 Translational Frequencies

The force components of a superconducting sphere is given by the code below. The forces are calculated and given by equation 2.34.

```
force[x_] := -(8*Pi r^3)/(3*mu0)*a1^2*
  x (*Force in the x direction*)

force[y_] := -(8*Pi r^3)/(3*mu0)*b1^2*
  y (*Force in the y direction*)

force[z_] := -(8*Pi r^3)/(3*mu0)*c1^2*
  z (*Force in the z direction*)
```

The spring constants are given by:

```
kx := (8*Pi*r^3)/(3*mu0)*a1^2
(*Spring constant in the x direction*)

ky := (8*Pi*r^3)/(3*mu0)*b1^2
(*Spring constant in the y direction*)

kz := (8*Pi*r^3)/(3*mu0)*c1^2
(*Spring constant in the z direction*)
```

The constants given above will give the following spring constants:

```
In[156]:= {kx, ky, kz}
Out[156]= {0.00124919, 0.0121662, 0.0212122}
```

As expected, the spring constants become higher in the order $k_x < k_y < k_z$. This is logical because the superconductor gets more pushed back in areas where the density is larger. Since the ellipse lies along the x axis, we expect it to push harder in the shorter y direction than the longer x direction. The magnetic field increases the most when we move along the z axis and therefore we expect this to have the highest spring constant.

We get the frequency out of the spring constant by:

$$f = \frac{1}{2\pi} \sqrt{\frac{k}{m}} \quad (4.4)$$

With the corresponding code:

```
fx := 1/(2*Pi)*Sqrt[kx/m] (*frequency in the x direction*)
fy := 1/(2*Pi)*Sqrt[ky/m] (*frequency in the y direction*)
fz := 1/(2*Pi)*Sqrt[kz/m] (*frequency in the z direction*)
```

And at last, the resulting frequencies are:

```
In[203]:= {fx, fy, fz}
Out[203]= {10.2701, 32.0506, 42.3206}
```

We also see here that the frequency in the z direction is the sum of the other two frequencies. This is explained by the fact that the slope of the magnetic field in the z direction is the sum of the other two slopes as seen in 4.3.

We take the z frequency from equation 2.35 and rewrite it:

$$f_z = \frac{|c|}{2\pi} \sqrt{\frac{2}{\mu_0 \rho}} = \frac{|a+b|}{2\pi} \sqrt{\frac{2}{\mu_0 \rho}} = \frac{|a|}{2\pi} \sqrt{\frac{2}{\mu_0 \rho}} + \frac{|b|}{2\pi} \sqrt{\frac{2}{\mu_0 \rho}} = f_x + f_y \quad (4.5)$$

And we see that the translational z frequency is indeed the sum of the other translational two frequencies.

4.3.2 Rotational Frequencies

Unfortunately, we have not been able to find the rotational frequencies. Nonetheless we can make assumptions on how to find these.

We can calculate the magnetic dipole moment by using the equation:

$$\vec{F} = \nabla(\vec{B} \cdot \vec{m}). \quad (4.6)$$

The magnetic dipole moment was also calculated this way in the thesis of T. De Jong and D. Kok [12], however there will only be a magnetic dipole moment when it is off-axis. Further calculations with these off-axis results will be difficult.

The next step is to calculate the torque exerted on the particle:

$$\vec{\tau} = \vec{m} \times \vec{B}. \quad (4.7)$$

The work the torque does is given by the integral:

$$W = \int_{\theta_1}^{\theta_2} \tau \, d\theta, \quad (4.8)$$

which is equal to the energy:

$$E_R = \frac{1}{2} I \omega^2. \quad (4.9)$$

Where I is the moment of inertia. The ω will be the rotational frequency.

Results and Discussion

5.1 The Lead Zeppelin Experiment

The whole dipstick for the new asymmetrical Lead Zeppelin is now finished. All the components are made to fit in the dipstick. The dipstick is airtight and gives no problems when sucking vacuum.

A lot of time was put in the big coil. The wire kept breaking and glue was accumulating on the wire which made it harder to wind. Optimal would be to have around 10.000 windings, but 6828 should in theory be enough.

Furthermore, five lead balls have been made for following experiments. These should be enough because they all have different properties.

The wires running through the big coil and elliptical coils have been measured and show a resistance in the right range. The resistance of the other wires have also been tested and they are all conducting with sensible resistances.

An effort has been made to make the components as invulnerable as possible. All the wires are put in teflon socks. The wires are then bounded together so no wire gets hooked behind something.

The Lead Zeppelin has three Faraday cages to reduce the EM noise.

The dipstick was carefully placed in a barrel of helium-4. The manometer showed a pressure of 10^{-3} millibar. The SQUID and voltage meter showed indications that the dipstick was not cold enough, so helium has been added to the inside of the dipstick. The pressure increased to 0.1

millibar. This did not make any difference.

The results on the computer showed that the voltage meter measures a charge build-up when the switch was still turned off. This means that the current flows through the elliptical coils instead of the shortcut. We have replaced the shortcut with a new niobium wire but the results stay the same. It could be the case that the shortcut is not cold enough to superconduct, but the reason has not been found.

5.2 Numerical Results

The magnetic field of the elliptical coils with $I = 0.25\text{A}$ is approximated by:

$$\vec{B}(x, y, z) = 7.90x\hat{x} + 24.66y\hat{y} - 32.567z\hat{z}. \quad (5.1)$$

With resulting frequencies: $f_x = 10.2701\text{ Hz}$, $f_y = 32.0506\text{ Hz}$ and $f_z = 42.3206\text{ Hz}$.

When we calculate the field for circular coils with a radius of \sqrt{ab} , so the areas stay the same, we get:

$$\vec{B}(x, y, z) = 15.42x\hat{x} + 15.42y\hat{y} - 30.83z\hat{z}. \quad (5.2)$$

With resulting frequencies: $f_x = 20.035\text{ Hz}$, $f_y = 20.035\text{ Hz}$, $f_z = 40.0686\text{ Hz}$.

For the ellipse, the field lines get squeezed in the y direction, and therefore loosened up in the x direction when we assume that the fluxes are the same. This explains the lower slope in the x direction, and higher slope in the y direction. This can also be mathematically verified by replacing a and b with \sqrt{ab} in equations 2.22, 2.23 and 2.24.

We see that we can distinguish the x and y frequencies even better by making the shape more elliptical, or in other words: increase the ratio $\frac{a}{b}$, where a and b are the elliptical properties.

By doubling the current to 0.5 Ampère, we get the following frequencies for elliptical coils: $f_x = 20.5402\text{ Hz}$, $f_y = 64.1012\text{ Hz}$ and $f_z = 84.6413\text{ Hz}$. We see that the frequencies get doubled, so the difference between f_x and f_y should also be twice as much. This property can be used for better distinguishing.

5.3 Fourier Spectrum of the Spherical Lead Zeppelin with Circular Coils

The Lead Zeppelin with elliptical coils has no results yet. Nonetheless, we could still look at the results of the circular Lead Zeppelin with a asymmetrical lead particle.

The Fourier Spectrum of the Lead Zeppelin with circular coils is given below.

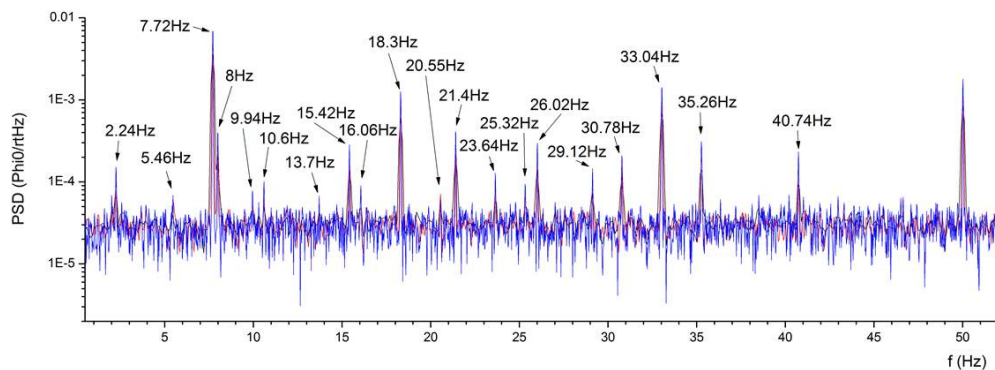


Figure 5.1: Frequency spectrum of an aspherical Zeppelin in between circular coils at 0.35 A right after a kick to the Dewar. We see many non-linearities from mixing and doubling frequencies.

With the 6 frequencies marked:

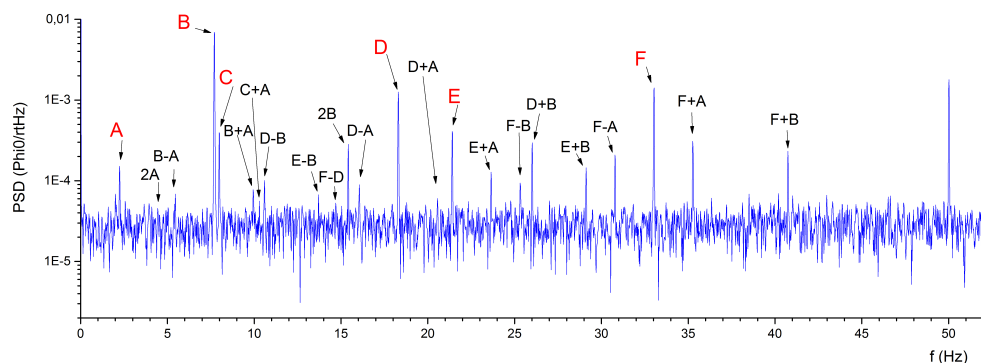


Figure 5.2: The frequency spectrum with its corresponding mixing and doubling frequencies.

We find the 6 frequencies by choosing sets. We choose fundamental frequencies as seen in the "calculated" row in figure 5.3. These frequencies show many similarities but other sets can always be chosen as fundamental frequencies.

height of peak	A	B	C	D	E	F
A	2A	A+B	A+C	A+D	A+E	A+F
B	B-A	2B	B+C	B+D	B+E	B+F
C	C-A	C-B	2C	C+D	C+E	C+F
D	D-A	D-B	D-C	2D	D+E	D+F
E	E-A	E-B	E-C	E-D	2E	E+F
F	F-A	F-B	F-C	F-D	F-E	2F
calculated						
	2,24	7,72	8	18,3	21,4	33,04
A	4,48	9,96	10,24	20,54	23,64	35,28
B	5,48	15,44	15,72	26,02	29,12	40,76
C	5,76	0,28	16	26,3	29,4	41,04
D	16,06	10,58	10,3	36,6	39,7	51,34
E	19,16	13,68	13,4	3,1	42,8	54,44
F	30,8	25,32	25,04	14,74	11,64	66,08
measured						
	A	B	C	D	E	F
A	4,44	9,94	10,3	20,55	23,64	35,26
B	5,48	15,42	15,84	26,02	29,12	40,74
C	5,76	0,33	16,06	26,34	29,49	41,02
D	16,06	10,6	10,3	36,62	39,74	51,34
E	19,14	13,7	E-C	E-D	2E	55,4
F	30,78	25,32	25,03	14,7	F-E	66,08

Figure 5.3: Part of the Excel file which includes data of the peaks

The yellow boxes are the frequencies which are in their error margins. The orange boxes show those outside their error margins. The red boxes are nowhere to be found. We can apply these peaks to the frequency spectrum and get figure 5.2 as result.

The translation frequencies in the x and y direction should be close together, in theory they should be at the same frequency. Therefore, it is logical to assume B and C are the translational x and y frequencies.

The frequency in the z direction must be twice as high, with closest frequency 15.42 Hz. However, this frequency does not show any mixing frequencies. The peak D shows more properties of a Zeppelin frequency,

therefore we assume D is the translational z frequency. However, this assumption is not mathematically verified.

Since we do not have a mathematical model for the rotational frequencies, we can only find these frequencies by reasoning. The only way to have a translational frequency around the z-axis, is to have inhomogeneities in the field. This creates a low frequency since these inhomogeneities are far lower than the change in magnetic field in other directions. Therefore, we assume that A is the rotational frequency around the z-axis.

This leaves us only with E and F for the other two rotational frequencies. The Zeppelin has a long and a short side, and wants to stay in one position since the potential must be the lowest in this position. Let us assume the longer side lies along the x direction. The rotation of the longer side, around the y-axis, has a bigger moment of inertia. This frequency must be therefore lower than the rotation frequency over the shorter side, around the x-axis. Peak E should be the rotation frequency of the longer side and F of the shorter side.

A higher current for this Lead Zeppelin has been used than the resulting frequencies of equation 5.2. However, the numerical frequencies are higher. A reason is that the field is approximated by loops which overlap at the same position, when in reality these loops are distributed over a length. The approximated loops are placed at the closest distance and therefore result in a higher magnetic field than the actual coils. An equation for the magnetic field for the loops distributed over the length of the coil can be calculated to make a more realistic approach.

Chapter 6

Conclusions

All the components are built, only the switch needs to be made to work. If this is done, one could most likely start to measure immediately. After this, we can look if the theoretical and numerical predictions are correct. The peak of the rotational frequency around the z-axis must shift to a higher frequency, the other rotational frequencies are now more defined by the elliptical properties and the translational frequencies should be better distinguishable.

There are many variables in this experiment, so it is better to put effort in experimenting instead of making more mathematical models. However, the results will make more sense if a model has been calculated for the rotational frequencies.

Follow up Experiments and Improvements

Since this experiment has just been built, it has a lot of room for follow up experiments and improvements. The most important follow up experiments are:

- *Getting the Lead Zeppelin to work properly.*
It is not clear if there are more problems with this new Lead Zeppelin project because it has not yet been put to the test. Maybe also other parts need replacement or optimization.
- *Calculating the rotational frequencies.*
The rotational frequencies have not yet been calculated and require a bit more work than the translational frequencies.
- *Comparing the results to the symmetrical Lead Zeppelin.*
In theory only differences between the frequencies should be shown. In reality there could be more differences and set backs.
- *Finding the corresponding frequencies.*
There is still some uncertainty about the which frequency correspond to which degree of freedom. The results get more clear when some experiments are done with a focus on connecting the frequencies to their degree of freedom.

Some improvements could be made like:

- *Finding equations for the distributed loops.*
The magnetic field of the coils has been calculated by assuming that the loops overlap at the same position. A better calculation takes care of this by distributing the loops over the length of the coil.
- *Finding the Taylor expansion of \vec{B} of the elliptical coils.*
The slopes of the magnetic fields should be a function of the variables used. The numerical approach is taken in this project, but a mathematical approach can also be done.
- *Distinguish the x and y frequencies better.*
This can theoretically be done by increasing the current or making more asymmetrical coils.
- *Finding the Q factor.*
The symmetrical Lead Zeppelin uses different material for the assembly of the coils and different Faraday cages. This can result in a different Q factor.
- *Putting the coils in a vibration-reducing cage.*
The symmetrical Lead Zeppelin now has a cage suspended by springs which reduces the mechanical noise from outside. This experiment could get the same cage built in when it proves its usefulness.

Acknowledgements

I would like to thank Tjerk Oosterkamp for granting me the opportunity to do this experiment. I think this was one of the few experiments this year which really sounded interesting to me. It has a good balance between the mathematics, hand crafting and computation. Every day had another goal (except the long period when I had to wind the big coil and it kept breaking) which really gave this experiment an adventurous feeling.

Also I would like to thank Bob for helping me out a lot in the beginning. The instructions for the experiment were always on point and you steered me every time in the right direction. That became clear when I tried to do the experiment alone and immediately cooked a barrel of helium.

Next, I want to thank everyone who provided me with information about this experiment. Including Martin de Wit, Tobias de Jong and David Kok. You did a great job writing all the necessary parts down.

I am grateful for everyone in the Interface Physics group for everything: from getting good coffee beans to helping me find stuff in the lab.

Outside the group I am indebted to the people of the FMD, especially Gert Koning, who literally made the whole experiment. There was always someone in the FMD who could help me with the material of the experiment.

Finally, I actually want to thank a lot of people for making this possible. My parents for helping me out, for providing me of a good environment and toasts. The students for making every day stressless. My friends outside the university for providing good energy after a long day. The

Netherlands for granting people the opportunity to get such good education. Tesla for the steady current flow through the lab. Bruch, Dvořák, Ray Charles and The Benny Goodman Orchestra for getting me through the long computation times. You have all been very lovely.

I am closing another chapter of my life and I am grateful that I am still motivated to learn more, even after all these years of school. I have learnt that good motivation comes from the small things like seeing your friends each day or listening to a great piece of music on the way home. I had a great time here at Leiden and hopefully see you all again.

Ian Berkman

References

- [1] C. L. Degen *et al.*, “Nanoscale magnetic resonance imaging,” *PNAS*, 2009.
- [2] O. Romero-Isart *et al.*, “Quantum magnetomechanics with levitating superconducting microsphere,” *Phys. Rev. Lett.* 109, 147205 (2012).
- [3] “Meissner effect.” [Online]. Available: https://en.wikipedia.org/wiki/Meissner_effect
- [4] M. de Wit, “The lead zeppelin project,” 2012.
- [5] D. J. Griffiths, *Introduction to electrodynamics*, 4th ed. Pearson, 2013.
- [6] “Superconductors.” [Online]. Available: <http://www.superconductors.org/INdex.htm>
- [7] “High-temperature superconductivity,” Helsinki University of Technology, Tech. Rep., November 2008.
- [8] M. Peiniger and H. Piel, “A superconducting nb3sn coated multicell accelerating cavity,” *IEEE Transactions on Nuclear Science*, vol. 32, no. 5, 1985.
- [9] R. Flükiger *et al.*, *Nb-Ti. 21b2: Nb-H - Nb-Zr, Nd - Np (The Landolt-Börnstein Database ed.)*. SpringerMaterials, 1994.
- [10] S. Westerdale, “Superconducting metals: Finding critical temperatures and observing phenomena,” MIT Department of Physics, Tech. Rep., April 2010.

- [11] E. Diez-Jimenez, J.-L. Perez-Diaz, and J. C. Garcia-Prada, "Local model for magnet–superconductor mechanical interaction: Experimental verification," *Journal of Applied Physics*, 2011.
- [12] T. de Jong and D. Kok, "Beweging van een supergeleidende bol in een anti-helmholtz-configuratie," January 2013.